This is a repository copy of *Permeability Prediction in Tight Carbonate Rocks using Capillary Pressure Measurements*.

White Rose Research Online URL for this paper:
http://eprints.whiterose.ac.uk/90927/

Version: Accepted Version

Accepted Manuscript

Permeability Prediction in Tight Carbonate Rocks using Capillary Pressure Measurements

F. Rashid, P.W.J. Glover, P. Lorinczi, D. Hussein, R. Collier, J. Lawrence
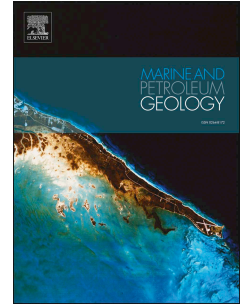
Please cite this article as: Rashid, F., Glover, P.W.J., Lorinczi, P., Hussein, D., Collier, R., Lawrence, J, Permeability Prediction in Tight Carbonate Rocks using Capillary Pressure Measurements, *Marine and Petroleum Geology* (2015), doi: 10.1016/j.marpetgeo.2015.10.005.

PERMEABILITY PREDICTION IN TIGHT CARBONATE ROCKS USING CAPILLARY PRESSURE MEASUREMENTS

Rashid, F.*, Glover, P.W.J., Lorinczi, P., Hussein, D., Collier, R., Lawrence, J.

School of Earth and Environment, University of Leeds, UK

* Email: eefnr@leeds.ac.uk, phone: +447445291315

Abstract. The prediction of permeability in tight carbonate reservoirs presents ever more of a challenge in the hydrocarbon industry today. It is the aim of this paper to ascertain which models have the capacity to predict permeability reliably in tight carbonates, and to develop a new one, if required. This paper presents (i) the results of laboratory Klinkenberg-corrected pulse decay measurements of carbonates with permeabilities in the range 65 nD to 0.7 mD, (ii) use of the data to assess the performance of 16 permeability prediction models, (iii) the development of an improved prediction model for tight carbonate rocks, and (iv) its validation using an independent data set. Initial measurements including porosity, permeability and mercury injection capillary pressure measurements (MICP) were carried out on a suite of samples of Kometan limestone from the Kurdistan region of Iraq. The prediction performance of sixteen different percolation-type and Poiseuille-type permeability prediction models were analysed with the measured data. Analysis of the eight best models is included in this paper and the analysis of the remainder is provided in supplementary material. Some of the models were developed especially for tight gas sands, while many were not. Critically, none were developed for tight gas carbonates. Predictably then, the best prediction was obtained from the generic model and the RGPZ models (R^2 = 0.923, 0.920 and 0.915, respectively), with other models performing extremely badly. In an attempt to provide a better model for use with tight carbonates, we have developed a new model based on the RGPZ theoretical model by adding an empirical scaling parameter to account for the relationship between grain size and pore throat size in carbonates. The generic model, the new RGPZ Carbonate model and the two original RGPZ models have been tested against independent data from a suite of 42 samples of tight Solnhofen carbonates. All four models performed very creditably with the generic and the new RGPZ Carbonate models performing well (R^2 = 0.840 and 0.799, respectively). It is clear from this study that the blind application of conventional permeability prediction techniques to carbonates, and particularly to tight carbonates, will lead to gross errors and that the development of new methods that are specific to tight carbonates is unavoidable.

35   KEYWORDS: capillary pressure, tight carbonates, permeability prediction, Kometan

36   limestone, Solnhofen limetone.

INTRODUCTION ACCEPTED MANUSCRIPT

Fluid permeability (Bernabé and Maineult, 2015) is one of the most important parameters in reservoir characterisation and management. While measurable on core samples in the laboratory, permeability is not available directly from downhole measurements. Since core sample measurement is expensive and core samples only cover a small proportion of any reservoir interval, other methods are required. Consequently, there exists a plethora of empirical models which have been designed to calculate permeability from a wide range of proxy measurements that often can be made downhole. We can classify these models into different types.

One common type relates the absolute permeability to the grain size, pore size or pore-throat size of the rock. These models can be considered to be percolation or characteristic length scale models and relate the progress of the fluid through a porous medium, which can be described by flow through an aperture with a single length scale. Examples of this include the Kozeny-Carman (*e.g*., Bernabé and Maineult, 2015, Schwartz *et al.,* 1986), Katz and Thompson (Katz and Thompson, 1986; 1987; Thompson *et al*., 1987) and RGPZ (Glover *et al.*, 2006) models. Walker and Glover (2010) considered the theoretical basis for all of these models.

A second common model treats flow paths in the rock as a bundle of tubes, each of which may have a different diameter. This is clearly a simplification of a porous medium, but it is a different simplification than that used by the characteristic length scale models. Some of these models include scaling coefficients, which enable this type of model to incorporate different connectivities. Such an approach is then beginning to converge with the electrical models represented by Archie's law (Archie, 1942), the modified Archie's law (Glover *et al*., 2000), and the generalised Archie's law for *n*-phases (Glover, 2010). Examples of this approach to permeability modelling include models by Swanson (1981), Wells and Amaefule (1985), Winland (Kolodzie, 1980), Huet *et al*. (2005), Pittman (1992), Kamath (1992) and Dastidar *et al*. (2007).

The main difference between the characteristic length scale (percolation) models and the Poiseuille-type models is that the latter defines and calculates the flow paths in the model exactly (as tubes) while the percolation models do not. Clearly, real rocks are rather more variable than the Poisseuille-type models assume, and that variability is built into the Poiseuille-type models by using empirical parameters that calibrate the model to a given formation in a given reservoir. Consequently, each calibrated prediction model is specific to a given reservoir, and errors would occur if the models were applied to another reservoir. This introduces an important restriction to the Poiseuille-type models which reduces their

72   generality. However, in conventional reservoirs, the restriction is often balanced by the

73   advantage that the quality of prediction in a well-calibrated formation of a particular reservoir

74   is often extremely good.

75   By contrast, the characteristic length scale models build the variability of the porous

76   medium into the model, describing flow through the medium in terms of a characteristic

77   length scale. Often these length scales have a single value, such as the modal pore diameter in

78   a pore size distribution of the rock. This can work well if the rock has a well-defined and

79   narrow unimodal pore diameter distribution, but works less well if the rock has a wide or

80   multi-modal pore diameter distribution. Sometimes such models are implemented using a

81   distribution of characteristic length scales. The RGPZ model (Glover *et al*., 2006), for

82   example, has been implemented in such a way that the overall permeability of a rock was

83   calculated from the geometric mean of the modal grain sizes weighted to account for the

84   distribution of those grain sizes within the rock (Glover *et al*., 2006). Such an approach

85   makes the often unjustified assumption that the whole range of grain (pore or pore throat)

86   sizes that are being averaged contribute to the permeability of the sample.

87   In this work almost all the models were developed initially for conventional reservoirs

88   with permeabilities greater than 1 mD (Comisky *et al*., 2007), although a few more recent

89   models, notably the Wells and Amaefule (1985) modification to the Swanson (1981) model

90   and the Huet *et al.* (2005) model were created specifically for tight gas sands with micro-

91   darcy permeabilities. None of the models tested in this paper have been developed for tight

92   gas carbonates with permeabilities in the nano-darcy to micro-darcy range. As far as we are

93   aware no models currently exist.

94

PERMEABILITY MODELS

96   The experimental data obtained in this study have been used to evaluate 16 permeability

97   models, which are listed in <u>Table 1</u>. In this table a distinction is made between empirical

98   constants, which are constants that have been obtained empirically but are not usually

99   allowed to vary in the application of the model, and fitting parameters, which are parameters

100 that are commonly expected to be varied in the application the model in order to make the

101 model fit the data.

102   Eight of the sixteen models which were tested performed very badly when predicting

103 the permeability of tight carbonate rocks. The description of these models and a full analysis

104 of how well they performed has been excluded from this paper, but included as a file of

105 supplementary material which can be downloaded from the publisher's website. The eight

106 models which are included in the supplementary material encompass the Katz-Thompson

107 models using critical lengths and electrical length models (Katz and Thompson, 1986; 1987;

108 Thompson *et al*., 1987), the Swanson model (Swanson, 1981), the Wells-Amaefule model

109 (Wells and Amaefule, 1981), the Kamath model (Kamath, 1992), the Huet et al. model (Huet

110 *et al., 2005*), and the Berg Fontainebleau model (Berg, 2014). Three of these models are of

111 the percolation-type, and the remaining five are of the Poiseuille-type.

112   All of the models listed in Table 1 can be implemented using data obtained from

113 MICP measurements. The fundamental underlying equation which governs the MICP method

114 is what we now call the Washburn equation (Washburn, 1921), which relates the capillary

115 pressure P_c in a capillary tube of radius R, containing air and mercury in terms of the

116 interfacial tension σ and the wetting angle θ.

117
$$P_c = \frac{2\sigma cos\theta}{R} \tag{1}$$

118 The Washburn equation should properly be called the Bell-Cameron-Lucas-Washburn

119 equation because similar theoretical developments had been made three years before by

120 Lucas (1918) upon work on capillary pressures by Bell and Cameron in 1906 (Bell and

121 Cameron, 1906). For mercury and air, the interfacial tension σ_{Hg-air}= 0.48 N/m (480

122 dynes/cm) and the contact angle $\theta_{Hg-air}=0^o$. In SI units, the use of R in meters gives the

123 capillary pressure in pascals. If imperial units are used, R in μm gives the capillary pressure

124 in psi.

125   Permeability is similar to electrical conductivity in that it can be thought of as being

126 partially controlled by the amount of pore space for hydraulic or fluid flow, and partially

127 controlled by how connected that pore space is (*e.g.,* Glover *et al*., 2015). The assumption

128 that underlies all of the permeability models is that there is a particular length scale, or

129 distribution of length scales, that controls the permeability of the rock. In the case of the

130 percolation models, that length scale is given explicitly in the model either as a characteristic

131 length scale with an undefined physical expression, as the mean, modal or median grain

132 diameter, as the pore diameter calculated with the theta transformation (Glover and Walker,

133 2009), or as some measure of the pore throat size such as that obtained from MICP

134 measurements.

135   In the case of the Poiseuille models, the capillary pressure that corresponds to a given

136 characteristic length through Eq. (1) is used. One must, therefore, chose which point on the

137 capillary pressure curve to use in order to define the capillary pressure for permeability

138 modelling. It is this capillary pressure will be associated with a particular wetting fluid

139 saturation (air saturation for MICP measurements, and usually water saturation in the

140 reservoir).

141   The most commonly used points on the capillary pressure curve are the entry pressure
142   and threshold pressure (Figure 1). The entry pressure on the mercury-injection curve is the
143   point on the curve at which mercury initially enters the sample. This point is often indicative
144   of the largest pore throat size present in the sample and is usually associated with the largest
145   pores (Robinson, 1966). There is some uncertainty that such a measure really does represent
146   the largest pore throat size because (i) we are limited to the sample size and larger samples
147   may contain larger pore throats, and (ii) irregularities on the surface of the samples can mimic
148   large pores and give erroneous results when Eq. (1) is applied to them. Consequently, the
149   low-mercury saturation portion of the MICP curve may not be truly representative of the rock
150   (Bliefnick and Kaldi, 1996).

151   The threshold pressure is that at which the saturation of mercury increases
152   dramatically and corresponds graphically to an upward convex inflection point on the
153   mercury-injection curve. It represents the capillary pressure at which the greatest population
154   of pore sizes fill and for a unimodal pore throat size distribution indicates the pressure at
155   which the mercury can for the first time access the pores which represent the main fraction of
156   porosity in the rock. This point has been used profitably by Dewhurst *et al*. (2002) to quantify
157   the capability of mud-rocks to trap high pressure fluids. The threshold pressure point has
158   been experimentally determined by recording electrical resistance across a sample and
159   measuring the pressures at which continuity occurs (Katz and Thompson, 1986; 1987;
160   Thompson *et al*., 1987).

161   Pittman (1992) and Winland (Kolodzie, 1980; Comisky *et al*., 2007; Gunter *et al*.,
162   2014) identified a mercury saturation percentile at which the reservoir threshold pressure can
163   be predicted to occur. Values of 3%, 5% and 10% (Schowalter, 1979) of the total mercury
164   saturation are considered by various researchers to predict the threshold pressure, although
165   such artificial restrictions are of no real utility since the threshold pressure depends upon the
166   rate of decrease of the tail of the pore throat size distribution which is sample-dependent.

167

168

169
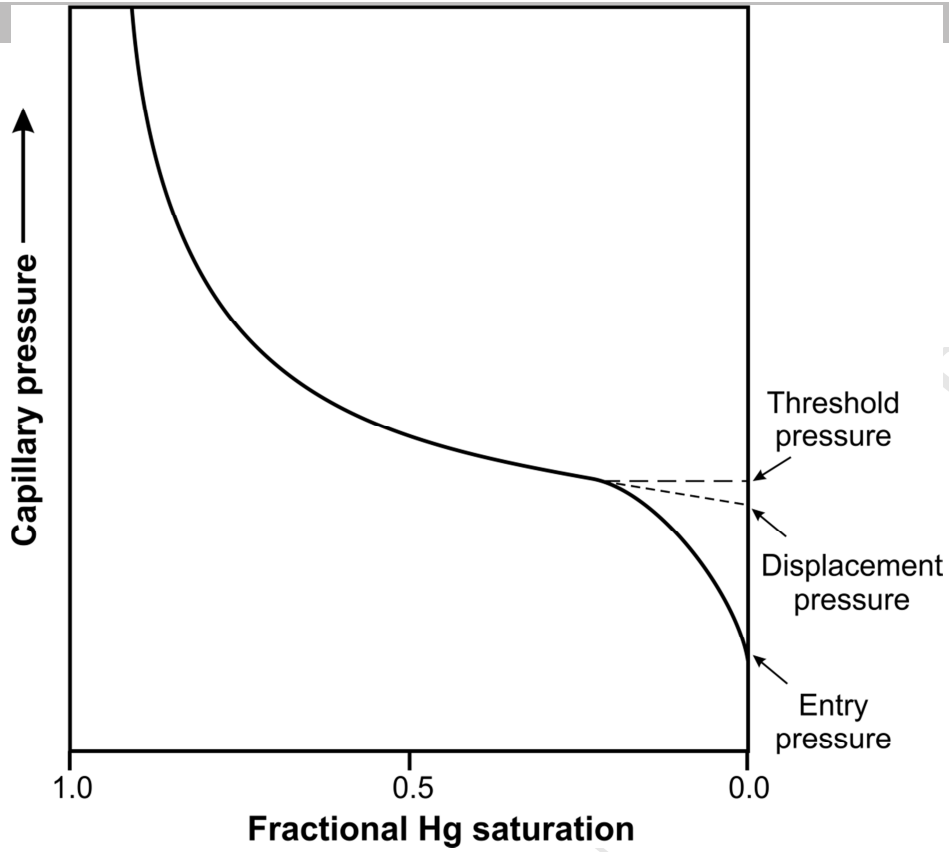
170   **Figure 1.** Definition of the entry pressure, displacement pressure and threshold pressure of a
171   MICP capillary pressure curve.

172
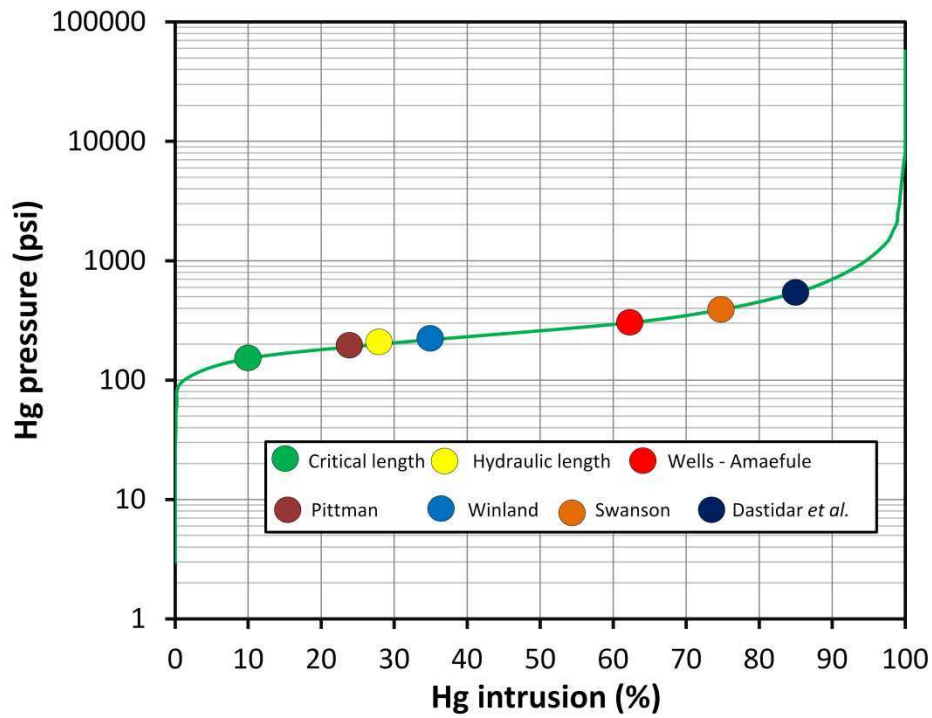
173   **Figure 2.** A typical capillary pressure curve for the MICP technique imposed upon which the
174   length scales from the various models are used in this work.

175 **Table 1.** Fundamental properties and inputs of the sixteen models evaluated in this study.

Name	Parameters	No. of empirical constants	No. of fitting parameters	Reference
Percolation-based models				
Katz and Thompson – Critical length	• Critical length, L_c • Formation factor	1	None	Katz and Thompson (1986; 1987), Thompson *et al.* (1987)
Katz and Thompson - Maximum electrical conductance length	• Maximum electrical conductance length, L_{Emax} • Critical length, L_c • Fraction of Hg-filled pore volume at L_{Emax}, S_{LEmax} • Porosity, ϕ	1	None	Katz and Thompson (1986; 1987), Thompson *et al.* (1987)
Katz and Thompson - Maximum hydraulic length	• Maximum hydraulic length, L_{Hmax} • Critical length, L_c • Fraction of Hg-filled pore volume at L_{Hmax}, S_{LEmax} • Porosity, ϕ	1	None	Katz and Thompson (1986; 1987), Thompson *et al.* (1987)
RGPZ theoretical approximate	• Characteristic grain diameter, d_{grain} • Cementation exponent, m • 'a'-parameter • Porosity, ϕ	1	None	Glover *et al.* (2006)
RGPZ theoretical exact	• Characteristic grain diameter, d_{grain} • Cementation exponent, m • 'a'-parameter • Formation factor F, or porosity ϕ	1	None	Glover *et al.* (2006)
RGPZ empirical carbonate	• Characteristic grain diameter, d_{grain} • Cementation exponent, m • 'a'-parameter • Formation factor F, or porosity ϕ	1	1	This work
Schwartz, Sen and Johnson (SSJ) generic form	• Characteristic pore size, Λ • Formation factor F	1	1	Johnson *et al.* (1986); Johnson and Schwartz (1989); Johnson and Sen (1988); Schwartz *et al.* (1989)
Berg (Fontainebleau implementation)	• Porosity, ϕ	4	4	Berg (2014) Equation (53)

8

Berg generic model	• Effective porosity, ϕ_s • Effective hydraulic tortuosity, τ_s • Constriction factor, C_s • Characteristic length L_h (equal to the radius of a capillary tube)	1	None	Berg (2014) Equation (32)
Poiseuille-based models				
Swanson	• Apex value of Hg saturation to capillary pressure	2	2	Swanson (1981)
Wells-Amaefule	• Apex value of Hg saturation to capillary pressure	2	2	Wells and Amaefule (1985)
Kamath 'model'	• Apex value of Hg saturation to capillary pressure	2	2	Kamath (1992)
Winland	• Length at which a mercury saturation is 35%, R_{35} • Porosity, ϕ	3	3	Gunter et al. (2014)
Pittman	• Radius associated with the critical length L_c, R_{apex} • Porosity, ϕ	3	3	Kolodzie (1980)
Dastidar et al.	• Weighted geometric mean of the pore size, R_{wgm} • Porosity, ϕ	3	3	Dastidar et al. (2007)
Huet et al.	• Displacement pressure, P_d • Irreducible water saturation, S_{wi} • Porosity, ϕ • Brooks-Corey parameter, λ	5	5	Huet et al.(2005)

176

177

178 **Table 1.** – cont.

9

179 **Percolation-based models**

180 <u>Katz-Thompson [KT] models (Maximum Hydraulic Length)</u>

181 The Katz and Thompson models (Katz and Thompson, 1986; 1987; Thompson *et al.*, 1987)

182 are based on percolation theory, and consider flow through a porous medium with random

183 microstructure and connectivity. Flow is considered to be controlled by a length scale. There

184 are three different length scales which are commonly used, each of which leads to a different

185 permeability prediction model; the Critical Length (L_c), Maximum Hydraulic Length (L_{Hmax})

186 and Maximum Electrical Conductance Length (L_{Emax}). The Maximum Hydraulic Length

187 (L_{Hmax}) is described here, while the remaining two models are describe in the file of

188 supplementary material.

189   The Maximum Hydraulic Length (L_{Hmax}) is defined as the effective pore throat

190 diameter corresponding to the highest hydraulic conductance. The value of L_{Hmax} is the length

191 corresponding to the capillary pressure at which the product of the mercury saturation and the

192 pore throat diameter, $S_{Hg} \times d_{pt}$, is maximum. Katz and Thompson introduced a permeability

193 model based on the length scale L_{Hmax} (Katz and Thompson, 1986; 1987; Thompson *et al.*,

194 1987).

$$k_{LH} = C_2 \left(\frac{L_{H\,max}^3}{L_c} \right) \phi \, S_{LH\,max} \quad , \tag{2}$$

196 where the term $L_{H\,max}^3 / L_c$ provides the length-squared dimensions required for permeability,

197 S_{LHmax} is the fraction of connected pore volume filled with mercury at L_{Hmax}, and the term

198 $\phi \, S_{LH\,max}$ represents the fraction of the whole rock filled with mercury at L_{Hmax}. The parameter

199 L_c is the critical length, which is defined as the critical pore diameter at which mercury forms

200 a connected path through the sample, as shown in <u>Figure 2</u>. This occurs at the threshold

201 pressure, which can be determined from the inflection point on a MICP curve. In this case the

202 constant $C_2 = 1013/89$. The constant has empirical origins but is usually not varied to

203 improve the fit or performance of the model.

204

205 <u>Schwartz, Sen and Johnson [SSJ] generic form</u>

206 A series of papers in the mid-80s (Johnson *et al.*, 1986; Johnson and Schwartz, 1989; Johnson

207 and Sen, 1988; Schwartz *et al.*, 1989) led to the development of a characteristic length scale

208 Λ for pores (Johnson *et al.*, 1986), and a new permeability model which used it. A

209 generalised form of this equation may be written as

210
$$k_{SSJ} = \frac{\Lambda^2}{aF},$$
(3)

211 where Λ is the Johnson *et al*. (1986) characteristic length scale of the pores, F is the

212 formation factor and a is a constant that may be treated as a fitting parameter (Walker and

213 Glover, 2010). This is an extremely simple model where the patency of the pores is expressed

214 by the length scale and the connectedness of the pore flow paths is expressed by $1/F$.

215 It should be noted that the characteristic length scale of the pores is not some measure

216 of the diameter or the radius of the pores in the usual sense; rather it is a measure of the effect

217 of the pores on defining the transport properties of the pore network.

218 We cannot implement the SSJ model directly with our dataset because of the

219 difficulty in finding an independent measurement of the characteristic length scale.

220 Furthermore, calculation of the Λ parameter from our grain size, cementation exponent and

221 formation factor would ensure that the SSJ model becomes formally the same as the RGPZ

222 model. Instead, we have used Eq. (2) to generate a generic permeability model which shares

223 some of the characteristics of both the SSJ and the RGPZ models. This equation may be

224 written as

225
$$k_{GENERIC} = \frac{d_{grain}^2}{bF^3},$$
(4)

226 where b is an empirically-determined parameter.

227 Walker and Glover (2010) took four of the most important models for predicting the

228 permeability of porous media; the classical model of Kozeny and Carman [K-C] (*e.g*.,

229 Bernabé, 1995), that of Sen, Schwartz and Johnson [SSJ] (Johnson *et al*., 1986; Johnson and

230 Sen, 1988; Schwartz *et al*., 1989; Johnson and Schwartz, 1989), that of Katz and Thompson

231 (Katz and Thompson, 1986; 1987; Thompson *et al*., 1987) [KT], and the RGPZ model

232 (Glover *et al*., 2006). Each of these models is derived from a different physical approach.

233 Walker and Glover (2010) rewrote them in a generic form which implied a characteristic

234 scale length and scaling constant for each model. After testing the four models theoretically

235 and against experimental data from 22 bead packs and 188 rock cores from a sand-shale

236 sequence in the U.K. sector of the North Sea, they concluded that the Kozeny-Carman model

237 did not perform well because it takes no account of the connectedness of the pore network

238 and should no longer be used.

239 They discovered that the other three models all performed well when used with their

240 respective length scales and scaling constants. Surprisingly, they found that the SSJ and KT

241 models produce extremely similar results and their characteristic scale lengths and scaling

242 constants are almost identical even though they are derived using extremely different

243 approaches: the SSJ model by weighting the Kozeny-Carman model using the local electrical

244 field, and the KT model by using entry radii from fluid imbibition measurements.

245

246 <u>RGPZ Model</u>

247 Like the SSJ model, the RGPZ model (Glover *et al.*, 2006a) is also derived analytically and

248 does not need calibration. The original equation is derived from the theoretical result that

249 links the characteristic length scale Λ introduced by Johnston *et al.* (1986) to permeability

250 through Eq. (2) and the approximate relationship between Λ and the electrical properties of

251 the porous medium $\Lambda \approx d_{grain}/2mF$. The result is

$$k_{RGPZ1} = \frac{d_{grain}^2 \phi^{3m}}{4am^2} = \frac{d_{grain}^2}{4am^2 F^3} , \tag{5}$$

253 where d_{grain} is some measure of the grain size which controls the flow properties of the

254 porous medium, m is the cementation exponent (dimensionless), and ϕ is the porosity (as a

255 fraction). It is important to note that the constant a is usually taken as 8/3 despite it being the

256 same parameter that appears in Eq. (2). Consequently, it may be left to vary, and if so, the

257 equation becomes empirical. It should be noted that this constant a is not the same as the

258 Winsauer et al. modification to Archie's law (see Glover, 2015).

259   It has been pointed out that Eq. (5) relies on the formation factor being much greater

260 than unity (*i.e.*, $F \gg 1$). While this is valid for clastic rocks without fractures, it may not be

261 the case for rocks with low values of F such as those containing significant fractures. An

262 exact form of the RGPZ equation, which is valid for all values of formation factor, can be

263 obtained by replacing the approximation $\Lambda \approx d_{grain}/2mF$ with its exact form

264 $\Lambda = d_{grain}/2m(F-1)$ (Revil and Cathles, 1999). This explains the failure of Eq. (5) for low F

265 and corrects it, leading to

$$k_{RGPZ2} = \frac{d_{grain}^2}{4am^2 F(F-1)^2} . \tag{6}$$

267 The definition of d_{grain} is critical to its implementation. For unimodal grain size distributions

268 the use of the simple modal grain size gives permeabilities that can be overestimated. Glover

269 *et al.* (2006b; 2006c) used Eq. (5) to compare the predictive powers of characteristic grain

270 size obtained from the (i) modal value, (ii) weighted arithmetic mean, (iii) weighted harmonic

271 mean, (iv) weighted geometric mean, and (iv) median values from grain size distributions

272   obtained from over 42 MICP measurements on glass bead packs, sands and reservoir rocks

273   over a range from 100 mD to 100 D. The mean values were weighted by the grain size

274   distribution across its entire range. The weighted geometric mean provided predicted

275   permeabilities that were closest to those measured.

276   While the RGPZ has no variable coefficients and is theoretical in nature, unknown

277   parameters such as, say, the cementation exponent, might be allowed to vary whereupon the

278   model would become empirical. This study recognises that the RGPZ model was developed

279   for clastic rocks and relies on their being a particular relationship between the grain size and

280   the pore and pore throat sizes that seem to hold for clastic rocks but not for carbonates. This

281   study has developed a new empirical permeability estimation method from the RGPZ model

282   which is described later.

283

284   <u>Berg (2014) Model</u>

285   Recently, Berg (2014) has published a new model that attempts to use parameters that are

286   both physically meaningful as well as being accessible experimentally. Berg's (2014) model

287   can be written as

288
$$k_{BERG2014} = \frac{\tau_s^2 L_h^2 \phi_s}{8C_s}, \tag{7}$$

289   where τ_s is the effective hydraulic tortuosity, L_h is the characteristic length relating to the

290   flow process and becomes equal to the radius in a capillary tube special case solution of the

291   equation, ϕ_s is the effective porosity, and C_s is called the constriction factor, and represents

292   how flow paths become constricted in the direction of flow just as the fluid passes from pores

293   into pore throats and out again.

294   The effective hydraulic tortuosity τ_s is the same as that used in the Kozeny-Carman

295   formulations which is represented as the shortest flow length possible (*i.e.*, the length directly

296   across the sample of rock) divided by the flow path length. This formulation of effective

297   hydraulic tortuosity leads to smaller values when the flow is contorted rather than direct. In

298   petrophysics we are more comfortable with the hydraulic tortuosity becoming larger if the

299   flow is more contorted, so we will use that definition instead, rewriting the hydraulic

300   tortuosity $\tau_h = 1/\tau_s$. Moreover, the electrical tortuosity is considered to be equal to the square

301   of this hydraulic tortuosity $\tau_e = \tau_h^2$ and the definition of electrical tortuosity is $\tau_e = F\phi$, which

302   allows Eq. (7) to be recast as

303
$$k_{BERG2014} = \frac{\phi^{1-m} L_h^2 (\phi - \phi_c)}{8 C_s} ,$$
(8)

304 where ϕ_c is the porosity that does not take part in fluid flow. We cannot determine ϕ_c and

305 have therefore taken $\phi_c = 0$. We have also assumed that the characteristic length L_h can be

306 represented by the Katz and Thompson hydraulic length L_{Hmax} used in Eq. (2). Taking all of

307 these modifications into account the Berg (2014) model implemented in our study under the

308 name of the 'Berg (2014) generic model' takes the form

309

310
$$k_{BERG2014} = \frac{L_{h\max}^2 \phi^{2-m}}{8 C_s} ,$$
(9)

311

312 where the constriction factor C_s is varied for the optimum fit, and hence the equation is used

313 by use as an empirical relationship.

314

315 **Poiseuille-based models**

316 <u>Winland Method</u>

317 The models of Swanson, Wells and Amaefule and Kamath are all, in effect the same,

318 differing only in the dataset upon which they have been calibrated. Winland, however,

319 introduced a new approach, where the length scale was that at which a mercury saturation of

320 35% is attained, or R_{35}. The value of R_{35} is simply the radius calculated using the Washburn

321 equation (Eq. (1)) from the capillary pressure corresponding to a mercury saturation of 0.35.

322 Winland recognised that the permeability was related to both R_{35} and the porosity ϕ with an

323 equation of the form

324
$$k_{Winland} = C_4 R_{35}^{a_2} \phi^{a_3} ,$$
(10)

325

326 where C_4, a_2 and a_3 are empirical variables, the permeability is calculated in mD and the R_{35}

327 value is in μm.

328   The Winland model was originally described as a series of three unpublished reports

329 for the Amoco Production Company, written between 1972 and 1976. These are consequently

330 difficult to obtain and not referenced in this study. Instead we reference studies by Kolodzie

331 (1980) and by Gunter *et al.* (2014), both of which discuss the Winland model in detail and the

332 latter of which gives the full references of the original three reports.

14

333   Winland calibrated his equation using a dataset consisting of 82 samples (56

334 sandstones and 26 carbonates) for which he had Klinkenberg-corrected permeabilities, and a

335 further 240 samples for which only uncorrected air permeability data was available. The

336 calibration gave $C_4 = 49.4$, $a_2 = 1.7$ and $a_3 = 1.47$. The range of the calibrating permeabilities

337 is unknown but we do know, thanks to the research of Comisky *et al.* (2007) that they were

338 made under ambient conditions.

339   The value of R_{35} is a rather crude way of defining the length scale that best

340 characterises fluid flow in a complex medium. Nevertheless, other constant values, such as

341 R_{40}, R_{50} have been suggested, but of those tested the R_{35} value, which corresponds to the

342 largest pore throat sizes has been found to give the best result (Nelson, 1994; Kolodzie, 1980;

343 Pittman, 1992).

344

345 <u>Pittman Model</u>

346 Pittman (1992) modified the Winland equation, using the length scale that corresponds to the

347 threshold pressure instead of R_{35}. This length scale is the same as the critical length scale

348 used by Katz and Thompson (Katz and Thompson, 1986; 1987; Thompson *et al.*, 1987), but

349 is used by Pittman as a radius. The Pittman equation is

350   $$k_{Pittman} = C_5 R_{Apex}^{a_4} \phi^{a_5} \quad . \tag{11}$$

351 Pittman calibrated this model using a set of 202 sandstone samples from 14 formations on

352 which measured permeability, porosity, and mercury injection data had been obtained

353 (Pittman, 1992) and obtained $C_5 = 32.3$, $a_4 = 1.185$, and $a_5 = 1.627$.

354   We have used our capillary pressure data to obtain a mean value for $R_{Apex} =$

355 0.135 ± 0.169, corresponding to a mercury saturation of 35%. In other words, the points shown

356 by the circles labelled Swanson and Winland in Figure 2 are very similar, and the two models

357 are sampling the same fraction of the pore space.

358

359 **Model summary**

360 There is a striking difference between the percolation models and those based on the

361 Poiseuille approach. The former need few empirical constants or sometimes none at all. The

362 latter need two or even three such constants. Consequently, it might be expected that the

363 Poiseuille-type models would provide better fits to data which are from similar formations,

364 due to their specificity and the advantage of having more fitting parameters. However, they

365 will perform much worse than the percolation models if they are used to predict the

15

366 permeability of rocks which do not share the characteristics of the rocks for which they were

367 calibrated.

368   Most of the models used in this paper were developed for use with clastic rocks, and

369 specifically for sandstone, with only a few being calibrated partially with carbonate samples.

370 Even the analytical RGPZ model was developed specifically for clastic rocks and has

371 traditionally not fared well in carbonates. The confining pressure of the measurements which

372 were used to calibrate the samples varied as well; from between 3000 to 4000 psi for the

373 model of Wells and Amaefule (1985) to only 800 psi or even ambient pressures in others

374 (e.g., Winland and Pittman). The permeability measurement approach also varied

375 significantly between all the models, including air permeabilities, steady-state and unsteady

376 state measurements, and pulse decay measurements. Some of these were corrected for

377 slippage, while others were not. Comisky *et al*. (2007) provide a useful table which compares

378 the experimental conditions of many of the permeability models listed above.

379   In other words, none of the methods summarised above were specifically derived for

380 tight carbonate rock samples (*i.e*., for permeabilities less than 1.0 mD). This study uses

381 samples with permeabilities in the range 100 nD to 0.7 mD, and which exhibit no fractures or

382 microcracks.

383

MATERIALS AND MEASUREMENTS

385 Two suites of samples were used in this work.

386   The initial assessment of all 16 of the models used a suite of 125 core plugs from the

387 Kometan formation, originating from different outcrop locations or core material from a

388 number of different fields in the western segment of the Zagros basin in the northern part of

389 Iraq (Rashid *et al*., 2015). For capillary measurements 25 plug samples were measured, of

390 which 3 failed to imbibe mercury because their pores were highly cemented. The effective

391 porosity of the samples ranged from 0.02 to 0.25, with a precision of ±0.005, while their

392 permeability ranged from 10 nD to 500 µD.

393   The validation testing on the newly developed RGPZ Carbonate model, the generic

394 model and the two original RGPZ models used a suite of 42 core plugs from the Solnhofen

395 limestone from a quarry near Blumenburg. The samples show a range of effective porosity

396 from 0.11 to 0.14 with a mean of 0.044, measured with a precision of ±0.005, and which had

397 a permeability range from 11.5 nD to 176 µD.

398   Prior to making any measurements, the cores were cleaned and dried using a Soxhlet

399   extraction process with low-temperature chloroform-methanol solutions according to the

400   American Petroleum Institute (API) recommended practices for core analysis. The samples

401   were then dried in a humidity-controlled environment. These cleaning and drying protocols

402   were initiated in order to reduce the effect of any damage or alteration of rock materials,

403   especially the clays that might enlarge pore spaces (Gant and Anderson, 1988).

404   The effective porosity of all the the Kometan samples was measured by helium

405   porosimetry using a Quantachrome stereopycnometer in the Wolfson Laboratory at the

406   University of Leeds, while the Solnhofen samples were measured using a high resolution

407   helium porosimeter that was designed and built by one of the authors of this paper and resides

408   in the Petrophysics Laboratory of the University of Leeds.The permeability of each sample

409   was measured using a helium pulse decay Klinkenberg-corrected permeability approach.

410   These measurements involve measuring the decay of gas pressure in an upstream reservoir as

411   the gas leaks through the sample. The measurements were carried out using a helium gas

412   pulse decay permeameter such as that in the Wolfson Laboratory of the University of Leeds

413   (Jones, 1997). At least four pulse decay tests were carried out for each rock sample, each with

414   different initial up-stream gas pressures in the range between 50 to 200 psi and downstream

415   pressures arranged such that the initial differential pressure was in the range of 5 to 40 psi.

416   All measurements of the Kometan limestone samples were made using a net confining

417   pressure of 800 psi, while all the Solnhofen samples were made at a net confining pressure of

418   725 psi, and at a temperature of 25° C in each case. The net confining pressure is very

419   important for tight rocks as permeability can vary greatly as a function of this parameter. All

420   permeability measurements were corrected for slippage effects as these can also be very

421   significant in tight rocks.

422   Considerable efforts were made to optimise the quality of these small porosity and

423   permeability measurements, including the preparation of high quality cylindrical core plugs.

424   The capillary pressure curve was measured using a high pressure mercury injection

425   capillary pressure technique, which involves injecting mercury into an evacuated core sample

426   in a stepwise fashion (Melrose, 1990). The volume of mercury injected at each pressure is a

427   measure of the non-wetting (*i.e.,* mercury) saturation. This method is relatively fast, usually

428   requiring only hours to complete each measurement. In addition, MICP techniques are

429   capable of applying injection pressures as great as 60,000 psi, which provides coverage of

430   almost the entire range of water saturation and capillary pressure for tight carbonate rock

431   samples, as well as for higher porosity and permeability reservoir quality rocks (Torsaeter

432 and Abtahi, 2000). The MICP technique has some disadvantages, which include the use of

433 mercury as a proxy for the reservoir non-wetting phase (usually a hydrocarbon) and air used

434 as the wetting phase, when in a reservoir it is usually water. Mercury-air capillary pressure

435 measurements made in this way require conversion to give the value they would have in a

436 reservoir using reservoir fluids and at reservoir pressure and temperature. This correction is

437 carried out using contact angle and surface tension measurements on the mercury-air-rock

438 system and on the reservoir fluid-rock system at reservoir conditions. Although the MICP

439 technique ensures that the sample cannot be used for further tests and must be disposed of

440 safely, the technique can be used on samples with irregular shapes, including drill cuttings

441 (Jennings, 1987). In this study tests were carried out using a MicroMeritics 33 Porotech IV

442 apparatus (Webb, 2001). The non-wetting phase was injected using 62 pressure steps which

443 were distributed logarithmically. The selection of penetrometer size is derived from the

444 combination of the sample volume and porosity (Giesche, 2006). Acceptable capillary

445 pressure results can be achieved when at least 20% of the penetrometer stem volume is

446 displaced into the rock sample. Tight rock samples with low porosities require larger sample

447 volumes for any selected penetrometer size. In this work penetrometers with stem volumes

448 between 0.392 cm^3 to 1.131 cm^3 were used. A mercury-air-rock contact angle of 140 degrees

449 and the mercury-air surface tension of 480 dynes/cm (0.48 N/m) (Webb, 2001) was used

450 throughout this work.

451 The MICP measurements were either used directly in modelling, which was usually

452 the case for the Poiseuille-based models, or were used to calculate a modal pore throat size

453 which could then be used to calculate a modal pore size or a modal grain size using

454 techniques of Glover and Déry (2010) and Glover and Walker (2009), respectively, for

455 subsequent use in modelling with the percolation-based models.

456 Some of the models also require the formation factor and cementation exponent to be

457 known. These were obtained by measuring the electrical properties of each of the samples

458 after they have been saturated with an aqueous solution. Full saturation of such tight samples

459 is a very difficult thing to carry out. In our case it involved a combination of evacuation and

460 saturation under a vacuum followed by pressurisation. The formation factor is best obtained

461 by making a number of electrical measurements while the rock is saturated with pore fluids

462 of different salinity. However, because the rocks are so tight we chose in all cases to calculate

463 the formation factor from the electrical resistivity measured on the rock at 1 kHz while it was

464 saturated with a single salinity of pore fluid together with the resistivity of that pore fluid.

465 The method for doing this is straightforward and can be found in the review by Glover (2015)

18

466 together with methods for measuring the resistivity of the pore fluid itself. A simple equation

467 links the cementation exponent to the formation factor and porosity, and hence the

468 cementation exponent for each sample can also be calculated simply, as also set out in Glover

469 (2015).

470 POROSITY & PERMEABILITY

471 Figure 3 shows a poroperm cross-plot of all the measured Kometan limestone data, some of

472 which was used in the initial modelling, as well as the Solnhofen data that was used as an

473 independent data set for testing purposes.

474 Figure 3a classifies the samples according to a petrofacies classification that is

475 discussed in Rashid *et al*. (2015). In this figure Petrofacies A is a compact

476 wackestone/packstone which has lost almost all of its primary porosity due to cementation,

477 containing nanometer-sized intercrystalline pores, and which contains occasional

478 microfractures and styllolites and consequently has a very low porosity and permeability.

479 Petrofacies B is a dissolved wackestone/packstone that contains moldic and vuggy pores, and

480 Petrofacies C is a carbonate mudstone that has undergone dissolution and possibly some

481 dolomitisation. Figure 4 shows typical scanning electronmicrographs for each petrofacies.

482 The petrophysical behavior of the samples is controlled by a complex pore geometry

483 system, governed by throat size, pore size and digenetic alteration. The poroperm diagram

484 shows each petrofacies distinctly. Petrofacies A comprises the first group and is well

485 separated from the other two petrofacies in the bottom, left-hand corner of the poroperm

486 diagram due to its low porosity and permeability, varying between 10 nD and 10 µD (green

487 symbols). This type of rock has porosities in the range 0.01 to 0.08 and a wide range of

488 permeabilities. The large spread of permeabilities reflects the large range of pore connectivity

489 present within this fabric, while the positive trend shows that any small increase in porosity

490 provides an enhancement of the connectivity of the pore network sufficient to increase the

491 permeability of the sample. There is some overlap between Petrofacies B and C (the blue and

492 red symbols in Figure 3, respectively), but both show significantly larger porosities and

493 correspondingly larger permeabilities. The relatively flat poroperm trend of Petrofacies C

494 shows that increasing porosity (in the range 0.18 to 0.28) is not significantly enhancing

495 permeability in the sample, which is in the range 0.08 to 4 mD. This agrees well with our

496 observation that moulds and vugs tend to be relatively unconnected to the pore network.

497 Petrofacies B has a well constrained porosity range, from about 0.08 to about 0.25, and an

498 equally well constrained permeability range. Overall there is a positive poroperm trend for

499 Petrofacies B, showing that higher porosities caused by dissolution also lead to higher

500 permeabilities (Rashid *et al*., 2015).

501
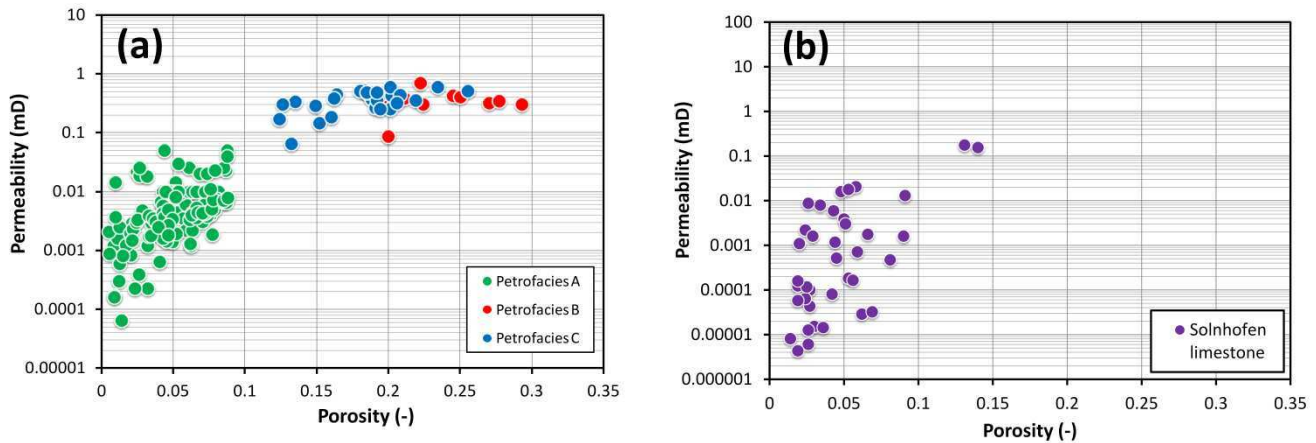
502

503

504 **Figure 3.** (a) Poroperm cross-plot of the three facies of Kometan limestone used in this

505 paper for initial testing of the 16 permeability models, and (b) Poroperm cross-plot of the

506 Solnhofen limestone data that was used as an independent data set for testing four of the

507 better-performing models including the newly developed RGPZ Carbonate model.

508

509 Figure 5 shows a plot of the capillary pressure type-curves, demonstrating the full

510 range of the capillary pressure curves within the Kometan limestone dataset. The entry

511 pressure and displacement pressure of each group varies. A high entry pressure was recorded

512 for all samples, reflecting the tightness of all of the samples.

513 From the examination of thin section and SEM results of the representative samples,

514 we see a trend of decreasing pore size with decreasing pore throat size implying increasing

515 entry capillary pressure values and decreasing permeability. However, there is no similar

516 relationship between the pore size and grain size. The moldic pores have greater diameter

517 because they are derived from the dissolution of foraminifer chambers. Consequently, there is

518 no relationship between the size of these large moldic pores and the modal grain size of the

519 rock. This observation allows us to predict that the models which were developed for clastic

520 rocks and in which there is an implicit assumption that the pore and pore throat size are

521 related to the grain size, such as the RGPZ model, may not perform well in carbonates in

522 general and specifically in tight carbonates.

523
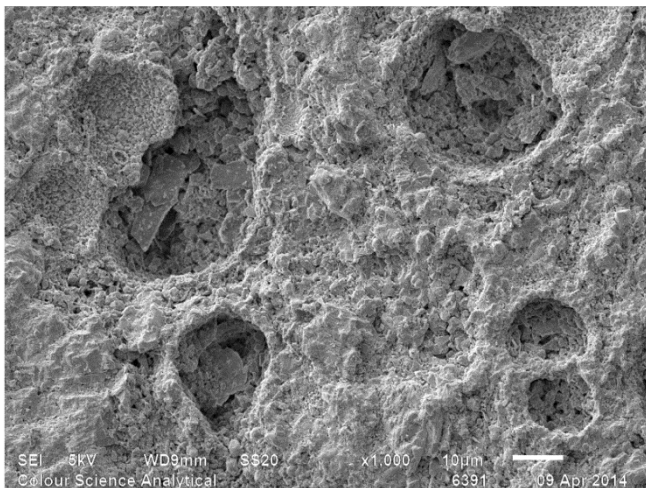
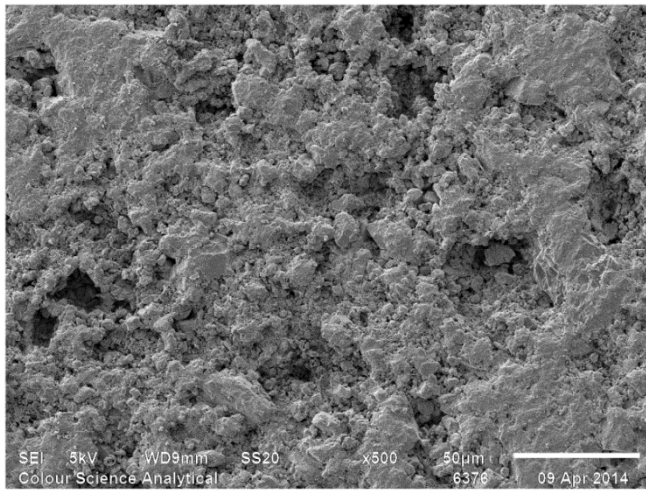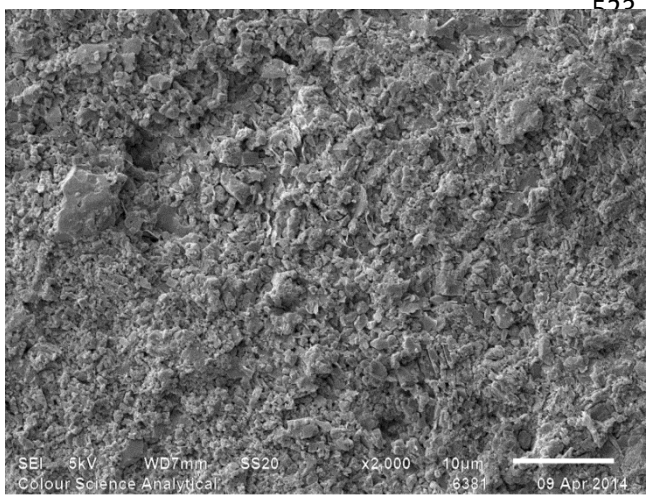Figure 3b shows the poroperm diagram for the Solnhofen limestone data, exhibiting a surprisingly large range of permeabilities for the zero to 0.1 porosity range. Many of these samples show a trend which overlaps that of Kometan limestone Petrofacies A.

Figure 4. Scanning electronmicrographs of the three facies of rocks studied in this work; Petrofacies A, upper; Petrofacies B, middle and Petrofacies C, lower.
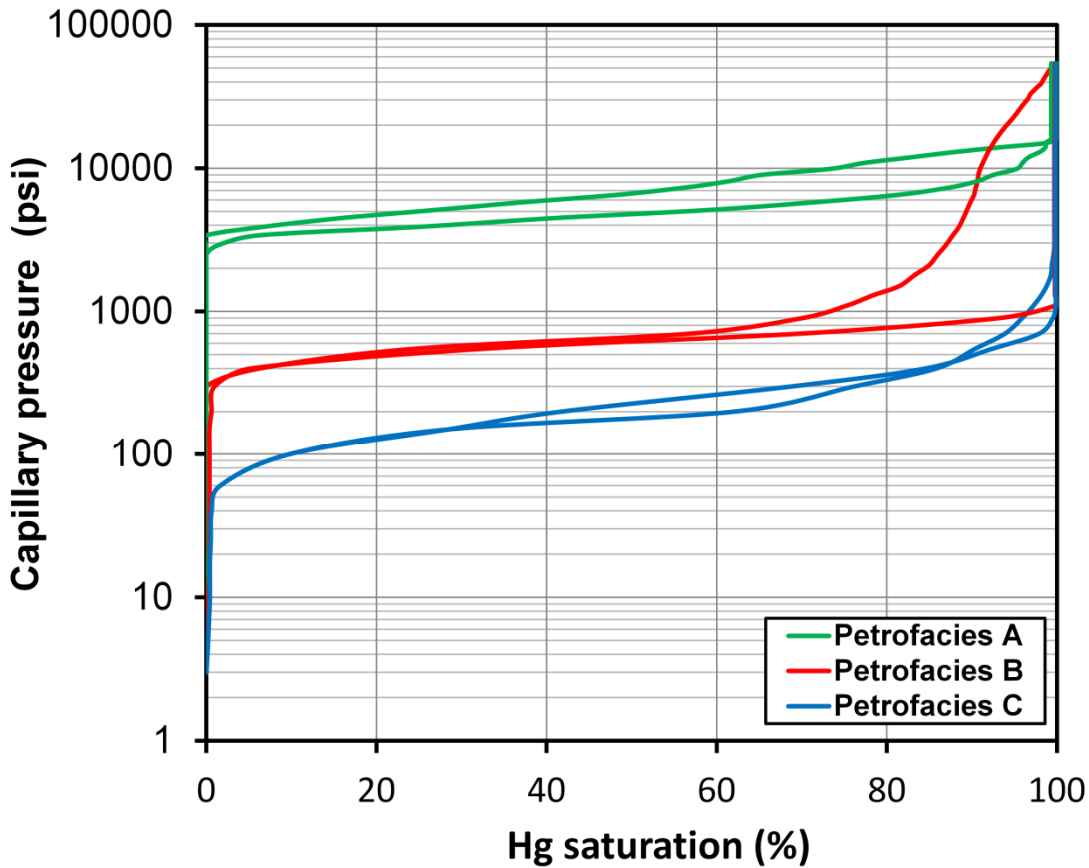
21

Figure 5. Mercury injection capillary pressure curves for typical samples from each of the three petrofacies used in this work.

A NEW MODEL FOR TIGHT CARBONATES

During our initial testing of the models with the Kometan limestone samples it became clear that a new and better model was needed for tight carbonate rocks, and we decided to try to develop one. Subsequently, this model was also tested with the Kometan limestone dataset, and then, as will be shown later in this paper, applied to another independent dataset of Solnhofen limestone.

In developing the new model we decided to take the theoretical RGPZ model as a starting point for a number of reasons. First, one of the authors had many years understanding the model having been one of those developing it initially. Second, the model has a theoretical pedigree so that any modifications made to ensure that it performs better in carbonate rocks can be understood as simple perturbations to an already well-understood relationship, rather than a complex interaction with previous empirical developments. Third, the model had shown itself to already be fairly good at predicting the permeability of

567 carbonate rocks, being ranked third and fourth of the sixteen models were initially tested.

568 Finally, it was thought that the reasons behind the failure of the RGPZ model in tight

569 carbonates was known, and might be corrected for by modification.

570   In clastic rocks there is a relationship between pore size and grain size. This arises

571 from the fact that clastic rocks are composed of eroded grains which are usually sub-

572 spherical. When the clastic rock contains some grains which have a plate-like shape, such as

573 micas, they are usually not present in a fraction sufficiently large enough to cause gross

574 changes to the microstructure of the pores. In this scenario, increasing the size of grains

575 clearly increases the size of the pores, and one might think that the pore throats would

576 increase in size as well. This idea has led to a mathematical transformation between pore size

577 and grain size for clastic rocks to be produced (Glover and Walker, 2009), where the

578 coefficient proportionality between the pore size and grain size is called the 'theta'

579 transformation, and depends upon the cementation exponent m, the formation factor F, and

580 the constant a=8/3. The relationship in clastic rocks between pore size and grain size holds

581 good providing there has not been significant diagenesis that alters the amount and

582 distribution of pore space within the rock.

583   In carbonates, however, it is common that there has been a large amount diagenesis,

584 which has altered the distribution of pore spaces within the rock by successive episodes of

585 dissolution, precipitation and recrystallisation. In this case, there is no simple or unique

586 relationship between grain size and pore size. Indeed, grains may be very large, complex and

587 interlocking with each other, while the pore spaces between them have small volumes and are

588 linked by tortuous pore throats. Increasing grain sizes are now not necessarily related to

589 increased pore sizes, and if they are the relationship will be very different to that for clastic

590 rocks. However, analysis of the results in this paper for the two conventional RGPZ models

591 shows them to do fairly well, but tend to overestimate the measured permeability. We

592 therefore hypothesise that we may get a much better prediction by scaling the theta

593 transformation, associating increases in grain size with smaller increases and pore size. The

594 RGPZ model uses a modal grain size as a length scale. However, it is a pore or pore throat

595 length scale that will ultimately control fluid flow. The implication is that we will still be able

596 to use an RGPZ-style model, with a grain size input parameter, for carbonate rocks but the

597 scaling factor will then take account of the fact that the input grain size is not necessarily

598 associated with pore size as large as it would be if the rock was a clastic rock.

599   The use of a grain size as an input parameter ensures that the RGPZ model is easy to

600 apply with widely available core data, but it implies that the RGPZ model incorporates a

23

601 relationship that converts, or interprets the grain size in a way which can influence a

602 predicted permeability as a pore or pore throat scale would. The question, therefore is

603 whether this internal relationship, which has been proven to work well for clastic rocks

604 (Glover *et al*., 2006) is also applicable to carbonates.

605 Consequently, we have produced a new model by taking the RGPZ exact model and

606 scaling the formation factor by an arbitrary factor η which is greater than unity, leading to a

607 larger formation factor than would be expected from the porosity and cementation exponents

608 of the samples. This process recognises that the connectedness of the pores involved in fluid

609 flow is less in carbonates than in a clastic rock of the same grain size. This process converts

610 the theoretical RGPZ model into an empirical model because the η-factor is now an

611 empirically-determined coefficient that can be viewed as a fitting parameter. The resulting

612 equation is

$$k_{RGPZCarbonate} = \frac{d_{grain}^2}{4am^2\eta F(\eta F - 1)^2} \approx \frac{d_{grain}^2}{4am^2\eta^3 F^3} . \tag{12}$$

614

615 The approximation is valid in the limit $F \gg 1$, and applies in this study because the formation

616 factors in tight carbonate rocks are generally very high, varying between 23 and 2565 with a

617 mean value of 314. The approximation will also be valid for most reservoir rocks, even those

618 with relatively high porosities.

619 Since the variation of η for individual samples would result in the trivial result of a

620 perfect prediction, we have shown the result for $\eta = 1.73$ in Figure 6f. This value was chosen

621 as the center of the range in which the fitting statistics were optimised. It is worth noting that

622 in the limit $F \gg 1$, the implementation of $\eta = 1.73$ is the equivalent of having a formation

623 factor or tortuosity that is 73% higher, a cementation exponent 9.53% higher (for $F = 314$), or

624 a grain, pore or pore throat size that is 43.9% of that assumed by the standard RGPZ model,

625 accounting for the observation that diagenetic processes in carbonates have reduced the

626 effective pore size with respect to the effective grain size.

627

PERMEABILITY PREDICTION

629 In total we tested 16 models and all are included in Table 1 for completeness. This number

630 includes the model that we have developed in this paper and describe later in the paper. Eight

631 of the models performed particularly badly when applied to tight carbonates. Consequently,

632 they are not reported in detail in this paper. However, their full description, concordance plots

633 and discussion is presented in a file of supplementary material available from the publishers

634 website. These models are those of the Katz-Thompson using critical lengths and electrical

635 length (Katz and Thompson, 1986; 1987; Thompson *et al*., 1987), the Swanson model

636 (Swanson, 1981), the Wells-Amaefule model (Wells and Amaefule, 1981), the Kamath

637 model (Kamath, 1992), the Huet et al. model (Huet *et al., 2005*), and the Berg Fontainebleau

638 model (Berg, 2014).

639   The remaining eight models, which are described further in this paper are the Katz-

640 Thompson model using hydraulic length models (Katz and Thompson, 1986; 1987;

641 Thompson *et al*., 1987), the Berg generic model (Berg, 2014), the Winland (Comisky *et al*.,

642 2007; Gunter *et al*., 2014) and Pittman models (Pittman, 1992), the exact and approximate

643 forms of the original RGPZ model, a generic form of the RGPZ/SSJ model (Glover *et al*.,

644 2006), and finally the model developed in this paper, which is a modification of the RGPZ

645 model for carbonate rocks, and which we have called the RGPZ Carbonate model.

646   Figure 6 shows how well each of the models predicts the measured permeability for

647 each sample of the Kometan limestone dataset. Each part of Figure 6 contains a 1:1 line that

648 indicates a perfect prediction as well as high and low bounds representing a variance of ±2.5

649 (i.e., upper and lower bounds representing 2.5 times greater or less than a perfect prediction,

650 respectively). A simple judgement concerning the goodness of prediction is that the

651 prediction falls between the variance ±2.5 limits.

652   Percolation-type models tend to perform better than Poiseuille-type models, with ony

653 two of the Poiseuille-based models performing well enough to be discussed in the main

654 paper. These are the models of Pittman and of Winland. Of the percolation models that did

655 not perform well, two only failed marginally – the critical length and electrical length models

656 of Katz and Thompson (Katz and Thompson, 1986; 1987; Thompson *et al*., 1987), while the

657 Berg (2014) model specific to Fontainebleau sandstone, unsurprisingly failed in carbonates.

658   The best performance was that of the Generic model and occurred for a value of

659 88<*b*<100. The new RGPZ empirical carbonate model also performed well with 1.7<η<1.76.

660 Both the exact and approximate forms of the standard RGPZ model (Glover *et al*., 2006) also

661 performed creditably, but produced a tendency to overestimate the permeability occasionally

662 by as much as an order of magnitude. Since the formation factors of tight carbonate rocks are

663 so high we might expect the two forms of the model to produce very similar results. This is

664 borne out by Figure 6. Calculation of the mean ratio of the permeability predicted using the

665 approximate form of the model to that using the exact form gives 0.979±0.0023, showing

666 how close the predictions are, and that the approximate form produces slightly lower
667 predicted permeabilities.

668   Of the Katz and Thompson (Katz and Thompson, 1986; 1987; Thompson *et al*., 1987)
669 models, the hydraulic conductivity model produced the best match with the measured
670 Klinkenberg-corrected permeability for these tight carbonates. However, while the general
671 trend of the permeability predicted with this technique matches the measured permeability
672 well, there is a large scatter and individual samples may have permeabilities up to an order of
673 magnitude larger or smaller than the real permeability.

674   The two best Poiseuille-based models were those of Pittman (Pittman, 1992;
675 Kolodzie, 1980; Comisky et al., 2007; Gunter et al., 2014) and of Winland (Gunter *et al*.,
676 2014), with the majority of the predictions falling within the ±2.5 variance criterion. The
677 Winland model is one of the simplest that we have, and it is instructive that it was calibrated
678 using Klinkenberg-corrected permeabilities. Nevertheless, the success of the Winland model
679 for our data and possibly other tight carbonates might rely on a happy coincidence that its use
680 of a mercury saturation of 35% upon which to base the length scale is close to the value for
681 rocks which share the texture (porosity and connectedness) of tight carbonates.

682   The Pittman model (Pittman, 1992) is a modification of the Winland model using a
683 length scale corresponding to the threshold pressure instead of R_{35}. For the rocks studied in
684 this work the Pittman model provided predictions of permeability that were a slight
685 improvement on those from the Winland model, over estimating permeability by about half
686 an order of magnitude. The use of the threshold pressure instead of R_{35} led, in our study to an
687 increase in the predicted permeability by a factor that was greater than unity in all but 3
688 samples and had an arithmetic mean of 2.62±1.31 using standard deviation to express the
689 uncertainty. It is clear from a comparison of these two models that, at least for the tight
690 carbonate rocks in our data, the length scale which controls the permeability of the rock
691 sample is closer to that associated with the threshold pressure than that associated with the
692 R_{35} point, and is larger than the length scale associated with the R_{35} point.

693
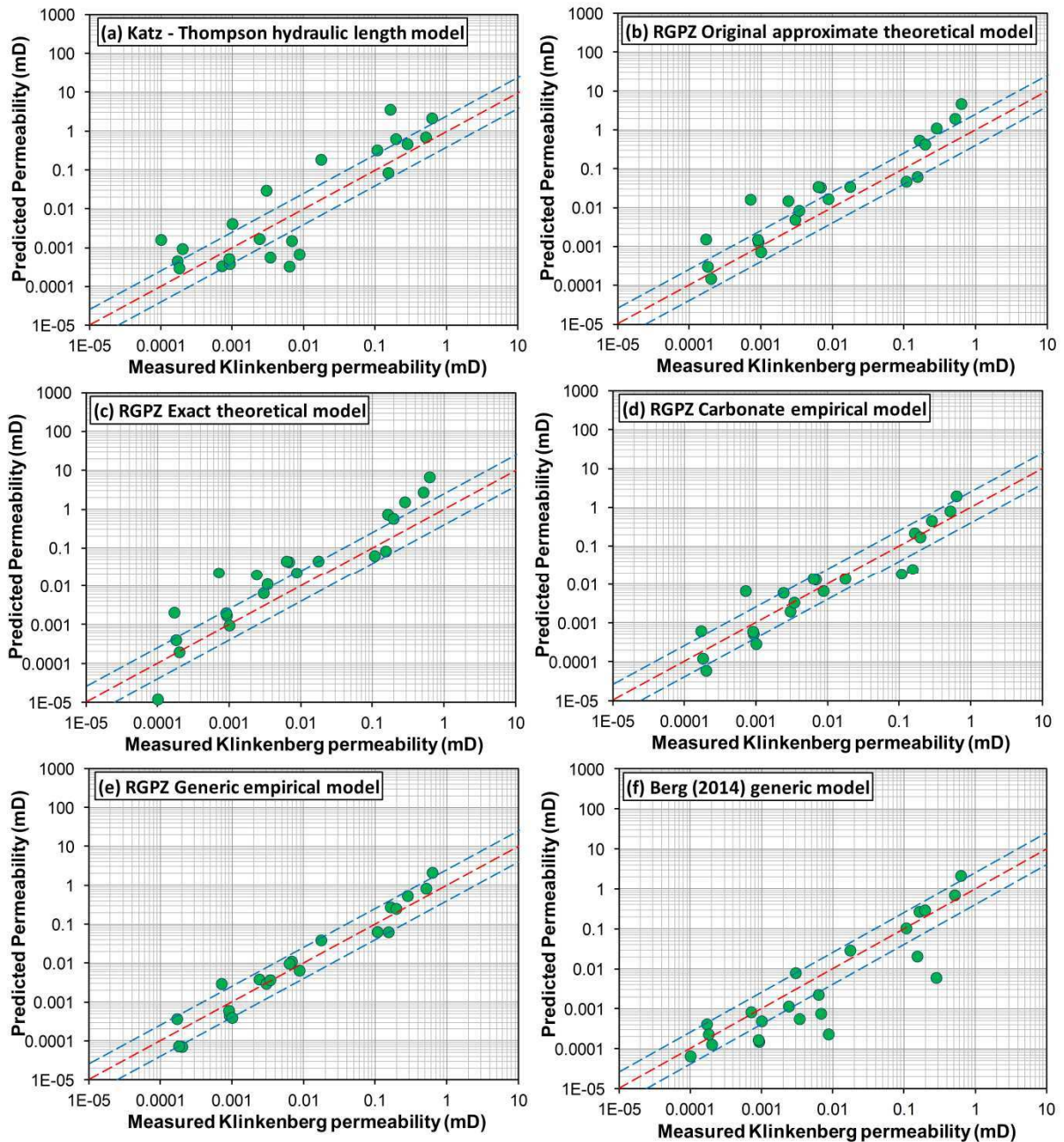
Figure 6. The performance of the 8 best models in predicting the permeability of a suite of Kometan limestone samples, together with a 1:1 perfect agreement and variance lines set at ±2.5. For (e) b=94, (d) η=1.73, and (f) C_s=3.4.

697

698
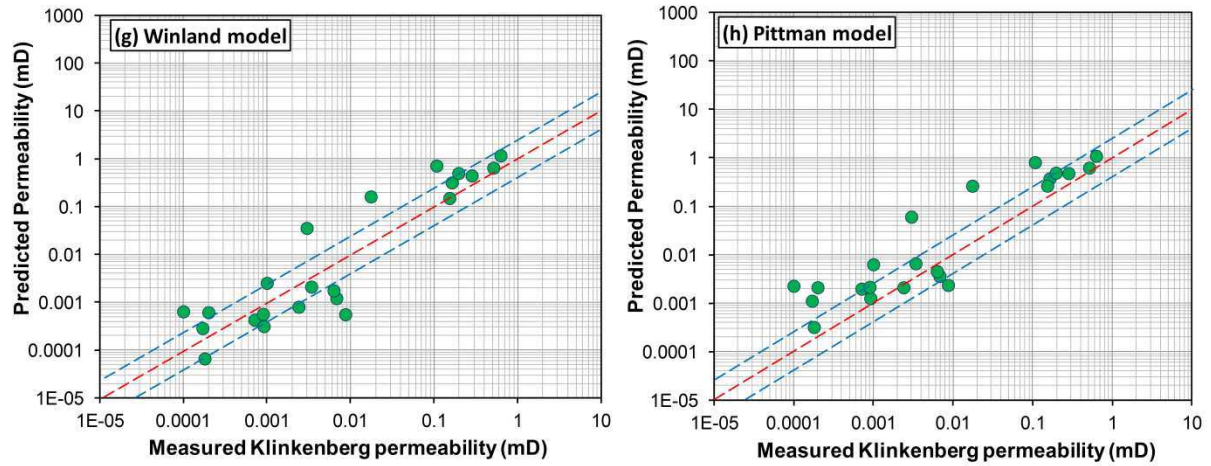
Figure 6. –cont.

700

701   We have quantified the performance of the prediction using three measures. These

702 are: (i) the percentage of samples with predictions falling within ±2.5 times the measured

703 permeability, to which we give the symbol ξ, (ii) the root mean squared residual of log values

704 (RMSLR), and (iii) the Pearson product-moment correlation coefficient (PPMCC). The

705 RMSLR is calculated using the equation

706
$$RMSLR = \sqrt{\frac{1}{n} \sum_{i=1}^{n} \left[\log(K_{L,i}) - \log(K_{est,i}) \right]^2}, \qquad \textbf{(13)}$$

707 where n is the sample population size, $K_{est,i}$ is the value of the predicted permeability, and $K_{L,i}$

708 is the measured Klinkenberg-corrected permeability.

709   Table 2 shows the prediction performance statistics for all 16 models, for

710 completeness. This table also gives a rank value for each test and an overall rank which is the

711 rank of the unweighted sum of the three individual ranks. On this basis the best two models

712 are the generic percolation model and the new RGPZ Carbonate model, and the worst two are

713 the Berg (2014) Fontainebleau model which is a percolation-based model calibrated for this

714 sandstone, and the Huet *et al*. model which is a Poiseuille-based model.

28

715 **Table 2.** Quantitative measures of permeability prediction effectiveness.

ξ (%)	Rank on ξ	RMSLR	Rank on RMSLR	PPMCC	Rank on PPMCC	Overall rank	Permeability model	Type
81.818	1	0.402	1	0.923	1	1	Generic model (Eq. (4))	Percolation
68.182	2	0.576	3	0.917	4	2	RGPZ empirical carbonate model	Percolation
54.545	5=	0.609	4	0.920	2	3	RGPZ approximate theoretical model	Percolation
54.545	5=	0.618	5	0.915	5	4=	RGPZ exact theoretical model	Percolation
59.091	3=	0.654	6	0.903	6	4=	Winland model	Poiseuille
40.909	7	0.576	2	0.872	7	6	Pittman model	Poiseuille
59.091	3=	0.696	7	0.858	10	7	Berg (2014) generic model	Percolation
31. 818	9	0.969	9	0.918	3	8	Katz and Thompson-Electrical length model	Percolation
36.364	8	0.724	8	0.575	14	9	Katz and Thompson-Hydraulic length model	Percolation
27.273	10	1.066	10	0.683	12	10	Katz and Thompson-Critical Length model	Percolation
4.545	13=	1.358	11	0.827	11	11	Wells and Amaefule model	Poiseuille
13.636	11=	1.605	12	0.613	13	12	Dastidar *et al*. model	Poiseuille
0.000	15=	1.976	13	0.866	9	13	Kamath 'model'	Poiseuille
0.000	15=	2.204	15	0.868	8	14	Swanson model	Poiseuille
13.636	11=	2.003	14	0.485	15	15	Berg (2014) Fontainebleau model	Percolation
4.545	13=	2.277	16	0.174	16	16	Huet *et al*. model	Poiseuille

ξ: Percentage of samples whose prediction is within a factor of ±2.5 of the real permeability.

RMSLR: Root mean squared log residuals, see Eq. (13).

PPMCC: Pearson product-moment correlation coefficient

29

TESTING THE NEW MODEL

716
717 Although the new RGPZ Carbonate model performed very well when predicting the
718 permeability of the Kometan limestone samples, we felt that it was necessary to validate the
719 new model by testing it against an independently obtained dataset. Consequently, we used a
720 dataset of 42 samples of Solnhofen limestone, which have already been described in an
721 earlier section of this paper. We did not restrict the permeability prediction to solely the new
722 RGPZ Carbonate model, but also carried out prediction with the two original RGPZ models
723 and the generic model. This was done so that the testing on the new RGPZ Carbonate model
724 could be viewed in the context of other well-performing models. It was particularly
725 interesting to us to see whether the modifications made to the existing RGPZ models made
726 any significant improvements when used in predicting the permeability of tight carbonates.

727
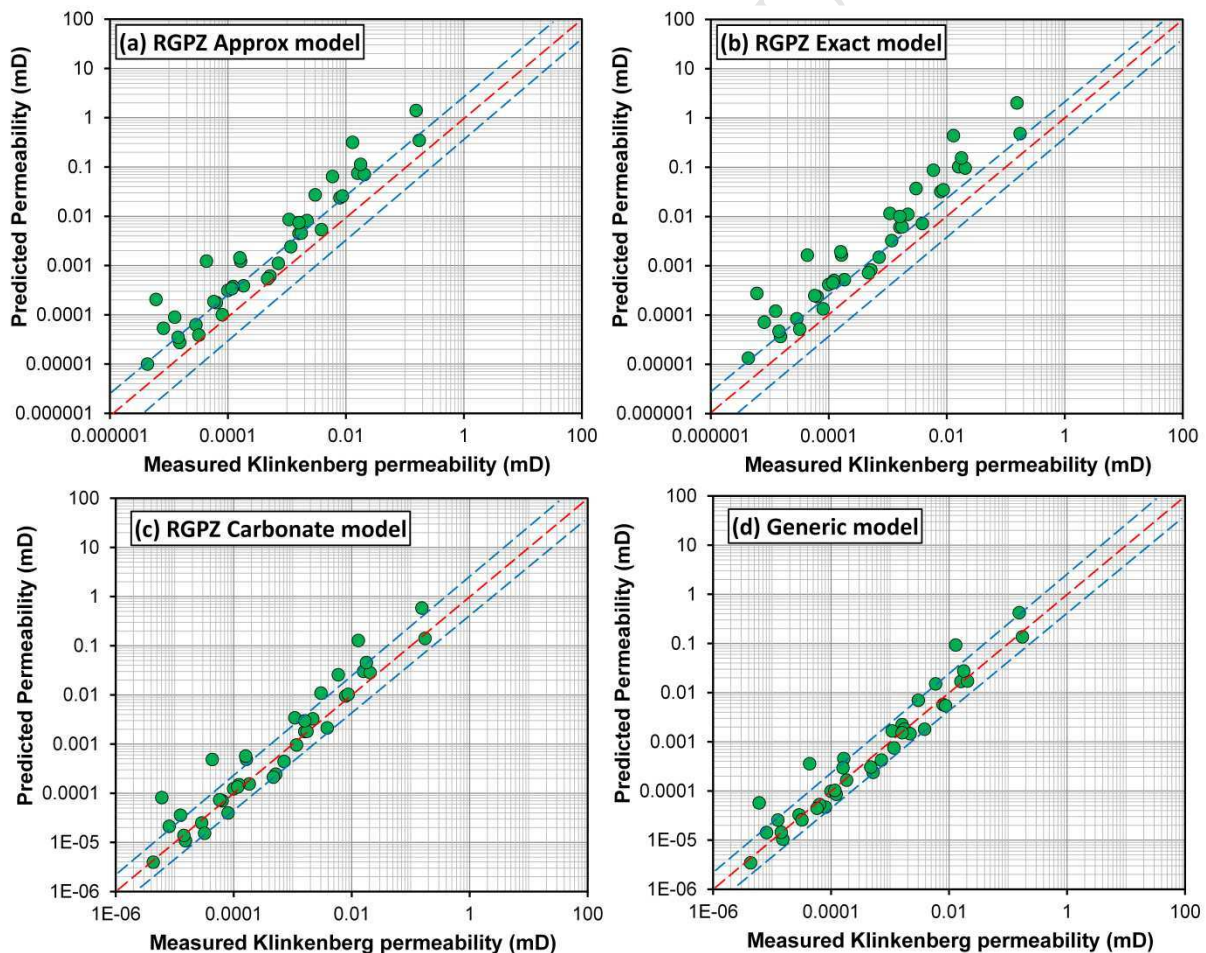
728

729 **Figure 7.** The performance of (a) the RGPZ approximate model, (b) the RGPZ exact model,
730 (c) the new RGPZ carbonate model and (d) the generic model, in predicting the permeability
731 of a suite of 42 Solnhofen limestone samples, together with a 1:1 perfect agreement and
732 variance lines set at ±2.5. For (c) η=1.5, and (d) b=100.

733

734   Figure 7 shows the results of the modelling. All four models performed creditably, but

735   once again the two original RGPZ models have a tendency to overestimate the permeability

736   in a subset of the samples. The Pearson product-moment correlation coefficient (PPMCC)

737   was 0.801 and 0.797, respectively. Both the new RGPZ carbonate model (PPMCC=0.799)

738   and the generic model (PPMCC=0.840) produced very good fits considering how small these

739   permeabilities are.

740   It should be noted that Figure 7 was produced by setting η=1.5, and b=100 for the

741   new RGPZ carbonate model and the generic model, respectively. These values could be

742   considered as fitting parameters, and varied to find the best fit for a particular rock type. We

743   have not attempt to do so, but doing so might improve the fit marginally in each case. The

744   value of these parameters depends upon how the grain size and pore throat sizes are

745   interrelated. Consequently, there is the potential for finding a physical control behind these

746   parameters in tight carbonates which would then allow them to be calculated independently.

747

748   ## DISCUSSION

749   All of the models considered in this study use MICP measurements to provide a length scale

750   from which a permeability can be calculated. In most cases, it is a single length scale that is

751   defined on the assumption that the pore throat size at a given mercury saturation is special in

752   that it represents the length scale that either controls or represents the permeability of the

753   rock. Different definitions are used by different models. However, given the great complexity

754   of rocks, it is unlikely that a length scale based on a single length measurement is likely to be

755   effective in describing the permeability of a range of different rocks.

756   Another approach calculates a single effective length scale from a weighted (usually

757   geometric) mean of all pore or pore throat sizes. The RGPZ method has been applied in this

758   approach fairly effectively (Glover *et al*., 2006a; 2006b; 2006c), and the method is used in

759   the method of Dastidar *et al*. (2007).

760   Whatever the method used to obtain the single, hopefully representative, value that is

761   to be used as a length scale, the fact remains that it is a single value, and much of

762   effectiveness of the prediction process depends upon it. In choosing a model, we are choosing

763   which definition of the length scale we think will produce the most accurate permeability

764   predictions.

765   Fourteen of the 16 models studied in this work contain coefficients that must be

766 obtained empirically. These models need to be calibrated against a typical dataset where the

767 permeability has been measured and is accurately known. It is important that these calibration

768 measurements are made on the same type of materials and under the same conditions as the

769 model will be applied. Consequently, the calibration for a tight carbonate should be carried

770 out on tight carbonates using Klinkenberg-corrected pulse decay gas pressure measurements

771 at a well-defined overburden pressure. These criteria were not fulfilled for any of the

772 empirical models tested. There were few calibration datasets that contained any carbonates

773 and there were no tight carbonates, while some calibration sets included tight clastic rocks.

774 Some calibration sets used gas permeabilities with undefined flow pressures, while others

775 used steady-state liquid permeabilities and a third group used unsteady-state pulse decay

776 measurements. In some of these measurements the flow pressures were not controlled, and

777 only a few calibration datasets had Klinkenberg-corrected their calibration data. Some

778 measurements were made at low equivalent overburden pressures, while others used a

779 consistent high value. In summary, the quality of the prediction depends upon the quality of

780 the calibration, and that was often very poor.

781   We associate the relative success of the Winland method with the fact that it was

782 calibrated with a suite of cores that contained a significant number of carbonates, that the

783 pulse decay permeability measurement was used and that all measurements were

784 Klinkenberg-corrected. In all of these respects the Winland model approaches the conditions

785 under which we measured our rock samples. It might be inferred, therefore, that the Winland

786 model's use of a pore throat radius being filled when 35% of mercury saturation is attained is

787 particularly valid for these tight carbonates. The slightly better predictions provided by the

788 Pittman approach might suggest that the threshold pressure is an even better characteristic

789 point upon which to base the pore throat scale length. The Katz-Thompson hydraulic length

790 characteristic method also provides acceptable permeability predictions for our tight

791 carbonate samples which implies that the highest hydraulic conductance of the Katz-

792 Thompson model is close to the R_{35} point for tight carbonate rocks. A cross-plot of the

793 permeability predicted using the Katz and Thompson model as a function of that predicted

794 with the Winland model shows a remarkable correlation with only a few samples not falling

795 on a 1:1 straight line.

796   The Dastidar *et al*. (2007) model is one of the more complex models tested. It applies

797 the weighted geometric mean approach that was used by Glover *et al*. (2006a; 2006b; 2006c)

798 with the RGPZ model. The concept in using this approach is that the permeability of the rock

799 is defined not by a single length scale, but by an ensemble of length scales from the very

800 largest to the very smallest according to how many pores of each size compose the rock. The

801 geometric mean is chosen because it represents the permeability of a random ensemble of

802 sub-volumes of the sample that have individual permeabilities. Consequently, using a

803 weighted geometric mean of the MICP pore throat sizes before applying the permeability

804 prediction equation is equivalent to calculating the permeability with the permeability

805 prediction equation for each pore throat size and then taking a weighted geometric mean of

806 the resulting permeabilities, providing the permeability prediction equation is linear. All of

807 the models investigated in this study fulfil this criterion.

808 Despite its complexity, the Dastidar *et al*. (2007) model did not perform well for tight

809 carbonates. This may be due partly to their use of sandstones, but the previously mentioned

810 averaging process may also be invalid in this application. It is interesting to note that the

811 weighted geometric mean length scale (R_{wgm}) that we calculated for each sample was always

812 significantly larger than R_{25} and R_{35}, which was the cause of the general overestimation of

813 permeability resulting from this model. This would then imply that the weighted geometric

814 averaging procedure was taking too much account of the largest pores in the rock. The

815 corollary is that the largest pores in tight carbonates do not contribute much to the overall

816 permeability of the rock, an observation that has been made previously by Rashid *et al*.

817 (2015). The implication is that the weighted geometric mean approach might work in tight

818 carbonates providing that the calculation was not done over the entire range of MICP data,

819 but ignores the largest pores. One might also make an argument for restricting the range of

820 the weighted geometric mean calculation to exclude the very smallest pores on the basis that

821 these small pores would have a capillary pressure too high for the pores to transmit fluids

822 under normal reservoir pressures.

823 Many of the more successful models that have been the subject of this paper use

824 electrical data in the form of the formation factor or the cementation exponent, or both. It is

825 interesting to ask the question whether these electrical data are accurate when made on tight

826 rocks. It is notoriously difficult to fully saturate a tight carbonate. The formation factor

827 measured on such a saturated tight carbonate will be that which relates to the pore network

828 that is saturated with pore fluid. If the entire pore network is not saturated with pore fluid the

829 measured formation factor will be higher than if it was completely saturated. It will be that

830 higher formation factor which will be used to predict permeability, and consequently the

831 predicted permeability will be lower than if the rock was fully saturated. The extent of this

832 problem is difficult to gauge, and it would be a useful subject to further study. One would

833 expect that there would be a systematic difference between the Klinkenberg-corrected

834 permeability measured on a tight carbonate rock with a gas like helium, which can percolate

835 through all of the pores no matter how small and the permeability measured with a liquid, and

836 one would expect the permeability predicted using a method that require the use of the

837 measured formation factor to also be smaller than the measured Klinkenberg-corrected gas

838 permeability.

839

840 ## CONCLUSIONS

841 There are many models that purport to be able to estimate or predict the permeability of rocks

842 for the purposes of reservoir characterisation, almost all of which were developed for high

843 porosity and high permeability conventional clastic reservoirs. However, the current need is

844 for models that will work in unconventional tight reservoirs which are often in carbonate

845 lithologies, with low permeabilities, and have a degree of heterogeneity and anisotropy.

846 A common approach to permeability prediction uses data from mercury injection

847 capillary pressure (MICP) measurements. We have taken sixteen MICP-based models and

848 have tested how well they predict the permeability of a suite of tight carbonate core plugs

849 from the Kometan formation in the north-east of Iraq. These include 7 existing percolation-

850 based models, 8 Poiseuille-based models, and a percolation-based model that we have

851 developed in this paper. We have included the full analysis of 8 of the models which show

852 the best performance in this paper, and have made available the full analysis of the remaining

853 eight in supplementary material which may be downloaded from the publisher's website.

854 All the permeability measurements presented in this paper were made by pulse decay

855 permeametry. All measurements were Klinkenberg-corrected, and were carried out at a fixed

856 overburden pressure of 800 psi for the Kometan limestone samples and 725 psi for the

857 Solnhofen limestone samples. Mercury injection capillary pressure measurements were made

858 on all samples. The permeability prediction methods often require supporting data such as

859 formation factor, and these were made independently.

860 It was expected that many of the models that were developed for high permeability

861 clastic rocks would fail badly when asked to predict the permeability of tight carbonates, and

862 this was indeed the case. In general percolation-based models performed much better than

863 Poiseuille-based models, though the Pittman model and Winland model performed creditably.

864 The best performing model was the simplest, being a generic model of the percolation type

865 upon which both the SSJ and RGPZ models are based, and both versions of the RGPZ model

866 also performed well. Consequently, we are led to the conclusions that (i) the blind application

867 of conventional permeability prediction techniques to carbonates, and particularly to tight

868 carbonates, will lead to gross errors, and (ii) the development of new methods that are

869 specific to tight carbonates is unavoidable.

870   There are many reasons why the predictions for many of the models are so bad. They

871 include:

872   1. The models were designed for high porosity and permeability clastic rocks.

873   2. The models were calibrated only in the high porosity, high permeability range.

874   3. The models were calibrated with data that had not been Klinkenberg-corrected.

875   4. The models were calibrated with data made at zero or uncontrolled overburden

876   pressures.

877   5. The models were calibrated using a mixture of permeability measurement approaches

878   including methods that are irrelevant to tight rocks.

879   6. Carbonate rocks do not have the same relationships between grain size, pore size and

880   pore throat size as clastic rocks due to their pore microstructure and particularly their

881   pore connectedness being affected by post-depositional diagenesis.

882

883   Consequently, we developed a new model based on the RGPZ theoretical model by

884 adding an empirical parameter to account for the relationship between grain size and pore

885 throat size in carbonates in an attempt to provide a better model for use with tight carbonates.

886 We have tested this new RGPZ Carbonate model, together with the generic model, and the

887 two original RGPZ models have been tested against laboratory permeability measurements

888 made on a suite of 42 samples of tight Solnhofen carbonate. In this dataset, the permeability

889 was measured using a Klinkenberg-corrected pulse decay technique at an overburden

890 pressure of 725 psi. These samples were also subjected to helium porosimetry, and electrical

891 measurements in order to obtain the formation factor and cementation exponents. Finally,

892 each sample was submitted to Mercury Injection Capillary Pressure measurements to obtain a

893 modal pore throat size, and modal pore sizes and grain sizes were calculated, providing a full

894 set of measurements required to predict the permeability using the four chosen methods.

895 All of the four models tested at this stage performed very creditably with the new RGPZ

896 Carbonate performing second best ($PPMCC = 0.799$). Perhaps surprisingly the best two

897 models, the generic model and the new RGPZ Carbonate model are also simplest, containing

898 only one empirical coefficient. It should also be remarked that the two original forms of the

899 RGPZ model, which also performed creditably, despite being strictly valid only for clastic

35

900 rocks, were the only theoretical models in the 16 tested, and consequently did not need to be
901 calibrated with experimental data.

902   In the light of needing to develop new and different ways to predict the permeability
903 of tight carbonates, it has been suggested that one approach might be to use multi-
904 dimensional imaging techniques such as CT scanning. If this were to be successful for tight
905 carbonates it would not only imply the use of extremely high-resolution CT scanning such as
906 that provided by NanoXCT imagers, but also the development of software that was capable
907 of reliably modelling fluid flow in the resulting digital pore microstructure model.

908

909 ACKNOWLEDGEMENTS

916

917 REFERENCES

918

919 ARCHIE, G.E. 1942. The electrical resistivity log as an aid in determining some reservoir
920   characteristics: Transactions of the American Institute of Mechanical Engineers, 146, 54–67.
921

922 BELL, J.M. & CAMERON, F.K. 1906. The flow of liquids through capillary spaces. J. Phys. Chem. 10:
923   658–674. doi:10.1021/j150080a005.
924

925 BERG, C.F. 2014. Permeability Description by Characteristic Length, Tortuosity, Constriction and
926   Porosity. Transport in Porous Media, 103(3), pp. 381-400.
927

928 BERNABÉ, Y. 1995. The transport properties of networks of cracks and pores. Journal of Geophysical
929   Research, 100(B3), pp. 4231-4241.
930

931 BERNABÉ, Y. & MAINEULT, A. 2015. Physics of Porous Media: Fluid Flow Through Porous Media. In:
932   Gerald Schubert (editor-in-chief) Treatise on Geophysics, 2nd edition, Vol 11. Oxford:
933   Elsevier;. p. 19-41.

934

935 BLIEFNICK, D.M. & KALDI, J.G. 1996. Pore geometry: control on reservoir properties, Walker Creek
936   field, Columbia and Lafayette Counties, Arkansas. *AAPG Bulletin,* 80**,** 1027-1044.

937

938 COMISKY, J.T., NEWSHAM, K., RUSHING, J.A. & BLASINGAME, T.A. 2007. A Comparative Study of
939   Capillary-Pressure-Based Empirical Models for Estimating Absolute Permeability in Tight Gas
940   Sands. Society of Petroleum Engineers.

941

942 DASTIDAR, R., SONDERGELD, C.H. & RAI, C.S. 2007. An Improved Empirical Permeability Estimator
943   From Mercury Injection For Tight Clastic Rocks.

944

945 DEWHURST, D.N., JONES, R.J. & RAVEN, M.D. 2002. Microstructural and petrophysical
946   characterization of Muderong Shale: application to top seal risking. *Petroleum Geoscience* 8**,**
947   371–383.

948

949 GANT, P.L. & ANDERSON, W. G. 1988. Core Cleaning for Restoration of Native Wettability.

950

951 GIESCHE, H. 2006. Mercury Porosimetry: A general (practical) overview. Particle & particle systems
952   characterization. 23**,** 9-19.

953

954 GLOVER, P.W.J. 2009. What is the cementation exponent? A new interpretation. Leading Edge
955   (Tulsa, OK), 28(1), pp. 82-85.

956

957 GLOVER, P.W.J. 2010. A generalized Archie's law for n phases. Geophysics, 75(6), pp. E247-E265.

958

959 GLOVER, P.W.J. 2015. Geophysical Properties of the Near Surface Earth: Electrical Properties. In:
960   Gerald Schubert (editor-in-chief) Treatise on Geophysics, 2nd edition, Vol 11. Oxford:
961   Elsevier; 2015. p. 89-137.

962

963 GLOVER, P.W.J., HOLE, M.J. & POUS, J. 2000. A modified Archie's law for two conducting phases.
964   Earth and Planetary Science Letters, 180(3-4), pp. 369-383.

965

966   GLOVER, P.W.J., ZADJALI, I.I. & FREW, K.A. 2006a. Permeability prediction from MICP and NMR data
967   using an electrokinetic approach. Geophysics, 71(4), pp. F49-F60.

968

969   GLOVER, P.W.J., ZADJALI, I. & FREW, K. 2006b. Permeability prediction from MICP and NMR data
970   using an electro-kinetic approach, Poster, EGU 2006, EGU06-A-01566, Vienna, 2-7 April
971   2006.

972

973   GLOVER, P.W.J., ZADJALI, I. & FREW, K. 2006c. A new equation for permeability prediction derived
974   from electro-kinetic theory., Oral, GAC-MAC-SEG-SGA 2006, Abstract No. 758, Montréal,14-
975   17 May 2006.

976

977   GLOVER, P.W.J. & WALKER, E. 2009. Grain-size to effective pore-size transformation derived from
978   electro-kinetic theory. *GEOPHYSICS,* 74**,** 17-29.

979

980   GUEGUEN, Y. & PALCIAUSAKAS, V. 1994. *Intoruction to the physics of rocks,* NJ, Princeton University
981   press

982

983   GUNTER, G.W., SPAIN, D.R., VIRO, E.J., THOMAS, J.B., POTTER, G., & WILLIAMS, J. 2014. Winland
984   Pore Throat Prediction Method - A Proper Retrospect: New Examples From Carbonates and
985   Complex Systems. Society of Petrophysicists and Well-Log Analysts SPWLA-2014-KKK, SPWLA
986   55th Annual Logging Symposium, 18-22 May, Abu Dhabi, United Arab Emirates.

987

988   HUET, C.C., RUSHING, J.A., NEWSHAM, K.E. & BLASINGAME, T.A. 2005. A Modified Purcell/Burdine
989   Model for Estimating Absolute Permeability from Mercury-Injection Capillary Pressure Data.
990   International Petroleum Technology Conference, Doha, Qatar, Nov. 21-23, Paper IPTC
991   10994.

992

993   JENNINGS, J.B. 1987. Capillary Pressure Techniques: Application to Exploration and Development
994   Geology. *AAPG Bulletin,* 71**,** 1196-1209.

995

996   JOHNSON, D.L., KOPLIK, J. & SCHWARTZ, L.M. 1986. New pore-size parameter characterizing
997   transport in porous media: Physical Review Letters, 57, no.20, 25642567,
998   doi:10.1103/PhysRevLett.57.2564

999

1000 JOHNSON, D.L., & SCHWARTZ, L.M. 1989. Unified theory of geometrical effects in transport

1001   properties of porous media: Presented at 30th Annual Symposium, Society of Petrophysicists

1002   and Well Log Analysts paper E, 1–25.

1003 JOHNSON, D.L., & SEN, P.N. 1988. Dependence of the conductivity of a porous medium on

1004   electrolyte conductivity: Physical Review B: Condensed Matter and Materials Physics, 37, no.

1005   7, 3502–3510, doi: 10.1103/Phys.RevB.37.3502.

1006 JONES, S.C. 1997. A Technique for Faster Pulse-Decay Permeability Measurements in Tight Rocks.

1007

1008 KAMATH, J. 1992. Evaluation of Accuracy of Estimating Air Permeability From Mercury-Injection

1009   Data.

1010

1011 KATZ, A.J. & THOMPSON, A.H. 1986. Quantitative prediction of permeability in porous rock. *Physical*

1012   *Review B,* 34**,** 8179-8181.

1013

1014 KATZ, A.J. & THOMPSON, A.H. 1987a. Prediction of rock electrical conductivity from mercury

1015   injection measurements. *Journal of Geophysical Research: Solid Earth,* 92**,** 599-607.

1016

1017 KOLODZIE, S., JR. 1980. Analysis Of Pore Throat Size And Use Of The Waxman-Smits Equation To

1018   Determine Ooip In Spindle Field, Colorado. Society of Petroleum Engineers.

1019

1020 LUCAS, R. 1918. Ueber das Zeitgesetz des Kapillaren Aufstiegs von Flussigkeiten. Kolloid Z. 23: 15.

1021   doi:10.1007/bf01461107.

1022

1023 MELROSE, J.C. 1990. Valid Capillary Pressure Data at Low Wetting-Phase Saturations (includes

1024   associated papers 21480 and 21618).

1025

1026 NELSON, P.H. 1994. Permeability-porosity Relationships In Sedimentary Rocks.

1027

1028 PITTMAN, E.D. 1992. Relationship of porosity and permeability to various parameters derived from

1029   mercury injection-capillary pressure curves for sandstone. *AAPG Bulletin,* 76**,** 191-198.

1030

1031   RASHID, F., GLOVER, P.W.J., LORINCZI, P., COLLIER, R., & LAWRENCE, J. 2015. Porosity and

1032   permeability of tight carbonate reservoir rocks in the north of Iraq, Journal of Petroleum

1033   Science and Engineering, 133, 147–161, http://dx.doi.org/10.1016/j.petrol.2015.05.009

1034

1035   REVIL, A. and, CATHLES, L.M. 1999. Permeability of shaly sands: Water Resources Research, 35, 651–

1036   662.

1037

1038   ROBINSON, R.B. 1966. Classification of reservoir rocks by surface texture. *AAPG Bulletin* 50**,** 547-559.

1039

1040   SCHOWALTER, T.T. 1979. Mechanics of secondary hydrocarbon migration and entrapment. *AAPG*

1041   *Bulletin,* 63.

1042

1043   SCHWARTZ, L.M., SEN, P.N. & JOHNSON, D.L. 1989, Influence of rough surfaces on electrolytic

1044   conduction in porous media: Physical Review B: Condensed Matter and Materials Physics,

1045   40, no. 4, 2450–2458, doi: 10.1103/PhysRevB.40.2450

1046

1047   SWANSON, B. F. 1981. A Simple Correlation Between Permeabilities and Mercury Capillary

1048   Pressures.

1049

1050   THOMEER, J.H.M. 1960. Introduction of a pore geometrical factor defined by the capillary pressure

1051   curve. *Pet. Tech***,** 73-77.

1052

1053   THOMPSON, A.H., KATZ, A.J., & RASCHKE, R.A. 1987. Estimation of Absolute Permeability from

1054   Capillary Pressure Measurements. Paper SPE 16794 presented at the 1987 SPE Annual

1055   Technical Conference and Exhibition, Dallas, TX, Sept. 27-30.

1056

1057   TORSAETER, O. & ABTAHI, M. 2000. *Experimental reservoir engineering laboratory workbook,*

1058   Department of petroleum engineering and applied geophysics, Norwegian University of

1059   Science and Technology, Trondheim, Norway, Lab rep.

1060

1061   WALKER, E. & GLOVER, P.W.J. 2010. Characteristic pore size, permeability and the electrokinetic

1062   coupling coefficient transition frequency in porous media, Geophysics, 75(6), E235-E246,

1063   2010. [pdf] , doi: 10.1190/1.3506561

1064

1065   WASHBURN, E.W. 1921. The Dynamics of Capillary Flow. *Physical Review,* 17**,** 273-283.

1066

1067   WEBB, P.A. 2001. An Introduction to the physical characterization of materials by mercury intrusion

1068   porosimetry with emphasis on reduction and presentation of experimental data. Norcross,

1069   Georgia.

1070

1071   WELLS, J.D. & AMAEFULE, J.O. 1985. Capillary Pressure and Permeability Relationships in Tight Gas

1072   Sands. Society of Petroleum Engineers.

1073

1074

Highlights

- The Kometan Formation classified as tight carbonate reservoir.

- 16 existing models of permeability prediction have been applied.

- The generic percolation model and the new RGPZ empirical are the two best percolation model of permeability prediction.

- The Winland and Pittman methods are the two Poiseuille-based models that are provided a good result.

PERMEABILITY PREDICTION IN TIGHT CARBONATE ROCKS USING CAPILLARY PRESSURE MEASUREMENTS: SUPPLEMENTARY MATERIAL

Rashid, F.*, Glover, P.W.J., Lorinczi, P., Hussein, D., Collier, R.
School of Earth and Environment, University of Leeds, UK
* Email: eefnr@leeds.ac.uk, phone: +447445291315

This document contains information about 9 permeability prediction models of the 16 which were tested during the work described in Rashid et al. "Permeability Prediction in Tight Carbonate Rocks using Capillary Pressure Measurements", but which were found to be sufficiently ineffective when applied to tight carbonate rocks to not warrant their inclusion in the main paper.

The supplementary information is structured in two parts. The first describes each of the models. The second describes a comparison of the use of these models with independently measured pulse-decay gas permeability measurements. This data may be merged with the data in the main paper to provide a comparison of the effectiveness of all 16 models included in the study.

PERMEABILITY MODEL DESCRIPTIONS

This section describes the models which were found to be relatively ineffective in predicting the permeability of tight carbonate rock samples.

Percolation-based models

Katz-Thompson models

The Katz and Thompson model is in fact three models, two of which are too ineffective in carbonates to be described in the main paper and hence are described here. Since all three models are related, all three models will be described in this section.

The Katz and Thompson models are based on percolation theory, and consider flow through a porous medium with random microstructure and connectivity. Flow is considered to be controlled by a length scale, one for each version of the model, and each is defined differently.

The first model is the Critical Length (L_c) model, where the critical length is defined as the critical pore diameter at which mercury forms a connected path through the sample, as shown in <u>Figure 2</u> of the main paper. This occurs at the threshold pressure, which can be determined from the inflection point on a MICP curve. This model was shown to be ineffective in carbonates and is not included in the main paper.

The second model uses a characteristic length called the Maximum Hydraulic Length (L_{Hmax}). This is defined as the effective pore throat diameter corresponding to the highest hydraulic conductance. The value of L_{Hmax} is the length corresponding to the capillary pressure at which the product of the mercury saturation and the pore throat diameter, $S_{Hg} \times d_{pt}$, is maximum. This model was shown to perform reasonably in carbonates and is included in the main paper.

The third model uses a characteristic length called the Maximum Electrical Conductance Length (L_{Emax}), which is the effective pore throat diameter where ionic conductance is maximized. It is evaluated as the length corresponding to the capillary pressure at which the product of the mercury saturation and the pore throat diameter cubed, $S_{Hg} \times d^3_{pt}$ is maximum. This model was also shown to be ineffective in carbonates and is not included in the main paper.

One might think that L_{Hmax} and L_{Emax} would be the same if the porosity and pore connectivity remained the same. However, there exist pore spaces within the rock that are patent to fluid flow but closed to electrical flow due to ionic exclusion processes, while others conduct electrically but have a capillary pressure too great for hydraulic flow. The efficacy of the hydraulic model over the electrical model for carbonates might indicate that electrical transport in carbonates and particularly in tight carbonates is more effective than hydraulic transport and consequently the electrical model underestimates the permeability in such rocks.

Consequently, there are at least three possible models for calculating the permeability using the Katz and Thompson approach (Katz and Thompson, 1986; 1987; Thompson *et al*., 1987). The first is using the critical characteristic length L_c, where

$$k_{LHc} = C_1 L_c^2 G = \frac{C_1 L_c^2}{F} \ , \tag{S1}$$

where the constant $C_1 = 1013/226$. The parameter G is the connectedness (Glover, 2009; 2010), which is the ratio of the conductivity of the rock fully saturated with a conducting fluid to the conductivity of that fluid and is the inverse of the formation factor defined by

Archie (1942). Consequently, $G = \sigma_0/\sigma_w = \phi^m$, where m is the cementation exponent. The cementation exponent in reservoir rocks can vary from about 1 for fractured rocks to over 4 for some carbonates and should always be measured rather than assumed because its presence as an exponent makes the connectedness and formation factor extremely sensitive to its value (Glover, 2015). It is worth noting that the dimensionality $[L]^2$ of permeability is accounted for entirely by the length squared term in Eq. (S1) because all other terms are dimensionless.

Katz and Thompson showed that it was possible to obtain the conductivity ratio from a combination of L_c, L_{Emax} and S_{LEmax} which is the fraction of connected pore volume filled with mercury at L_{Emax} according to $G = \sigma_0/\sigma_w = L_{E\max} \phi S_{LE\max}/L_c$, allowing a new model for permeability to be written

$$k_{LE} = C_1 L_c L_{E\max} \phi S_{LE\max} \ , \tag{S2}$$

where the term $L_c L_{E\max}$ provides the length-squared dimensions required for permeability and the term $\phi S_{LE\max}$ represents the fraction of the whole rock filled with mercury at L_{Emax}. This is the Katz and Thompson electrical model.

Katz and Thompson also introduced a third model based on the hydraulic length scale L_{Hmax}

$$k_{LH} = C_2\left(\frac{L_{H\max}^3}{L_c}\right)\phi S_{LH\max} \ , \tag{S3}$$

where the term $L_{H\max}^3/L_c$ provides the length-squared dimensions required for permeability, S_{LHmax} is the fraction of connected pore volume filled with mercury at L_{Hmax}, and the term $\phi S_{LH\max}$ represents the fraction of the whole rock filled with mercury at L_{Hmax}. In this case the constant $C_2 = 1013/89$. It is this last model that performs best in carbonates and that is included in the main paper.

Comisky *et al.* (2007) have noted that all of the Katz and Thompson models are analytically derived and do not depend upon calibration to a given dataset even though Katz and Thompson did compare their models to experimentally derived data over the range 5 μD to 5 D with some success.

Berg Fontainebleau Sandstone Model

Berg implemented a version of their model as an empirical fit valid for Fontainebleau sandstone (Berg, 2014). While it was not expected that this version of the model would

perform well for tight carbonates, and indeed does not, we have implemented this model under the name 'Berg Fontainebleau model'. It is given by

$$k_{BERGFont} = 1329(\phi - 0.054)^{2.12}(\phi - 0.030).$$ **(S4)**

Poiseuille-based models

<u>Swanson Model</u>

Swanson (Swanson, 1981) proposed a permeability model where the permeability is controlled by a single point on the capillary pressure curve that is characterised by the apex of the plot of mercury saturation as a function of mercury saturation S_b, and which shares a great similarity to the equation of Thomeer (1960). The general formula used by Swanson is given by

$$k = C_3 \left(\frac{S_b}{P_c} \right)_{Apex}^{a_1},$$ **(S5)**

where C_3 and a_1 are empirically-determined constants. Swanson determined the constants by calibrating Eq. (S4) with data from 319 gas measurements on sandstone and carbonate rocks (203 clastic samples from 41 formations, and 116 carbonate samples from 330 formations) with a range of permeabilities from 20 µD to 2 D, and which were not Klinkenberg corrected, to obtain $C_3 = 399$ and $a_1 = 1.691$. It was recognised that such a correlation would be dependent on the sample set and that it would be particularly prone to error in tight rocks where slippage effects are more prevalent. Consequently, Swanson (1981) carried out a smaller calibration using 24 clean samples of sandstone upon which steady-state brine permeability was measured under a net stress of 1000 psi, to obtain $C_3 = 431$ and $a_1 = 2.109$.

It should be noted that the general equation used by Swanson (1981) (Eq. (S5)) is formally the same as the Katz and Thompson (Katz and Thompson, 1986; 1987; Thompson *et al*., 1987) electrical length scale model (Eq. (S2)), but gives different values of permeability when implemented because the Swanson version depends upon the Swanson calibrations.

<u>Wells-Amaefule Model</u>

The method of predicting permeability from capillary pressure proposed by Wells and Amaefule (1985) represents a modification and extension to the approach of Swanson (1985)

with technical improvements to the approach for determining the apex value and a calibration to tight sandstones. Wells and Amaefule (1985) calibrated the general Swanson equation with 35 samples of tight sandstone from two formations that varied between 20 nD and 70 mD, making their measurements under pressures between 3000 and 4000 psi using a gas pulse decay method with corrections for slippage and net overburden effects, obtaining the parameters in Eq. (S5) as $C_3 = 30.5$ and $a_1 = 1.56$. The Wells-Amaefule is best regarded as the same as the Swanson model but with some technical modifications and a different calibration designed to perform better in tight gas sands.

Kamath 'Model'

More recently Kamath (1992) has aggregated data from a number of different datasets including those of Katz and Thompson (1986), Swanson (1985) and Wells and Amaefule (1985) as well as some newly measured values to provide a new dataset for calibrating permeability models. The new dataset had 454 samples covering a very large range from 20 nD to 2 D. Despite the very large range of the measurements, their varied measurement methods; some being steady-state gas, some steady-state brine, some pulse-decay, and the awkwardness of some being corrected for slippage and net overburden while others were not, Kamath (1992) propose their model as valid for tight gas sands. After calibration with the dataset the Kamath model is given by Eq. (S5) with $C_3 = 413$ and $a_1 = 1.85$. The Kamath 'model' is, in fact, a misnomer. It is simply the Swanson model but calibrated with a larger dataset that is not self-consistent.

Dastidar *et al*. Model

Dastidar *et al*. (2007), have provided a model that looks very similar to that of Winland and is given by

$$k_{Dastidar} = C_6 R_{wgm}^{a_6} \phi^{a_7} \ . \tag{S6}$$

The main difference is in the value of R_{wgm}. Dastidar *et al*., (2007) followed the approach of Glover *et al.* (2006a; 2006b; 2006c) in calculating the characteristic length scale from the weighted geometric mean of a length scale distribution. In the case of Glover *et al.* (2006a; 2006b; 2006c) it was the weighted geometric mean of the grain diameter that was used in the RGPZ model. Dastidar *et al*., (2007) calculated the weighted geometric mean of the pore size from MICP data. In both cases, the weighted geometric mean describes the mixing of

randomly arranged arbitrary shaped sub-volumes of the rock, each characterised by a single size on the respective distribution, and each of a volume given by the weighting. The weighted geometric mean is best computed in logarithmic space in order to avoid runaway inflation of the product, and is given by

$$\ln\langle x\rangle_g = \sum_{i=1}^{N} w_i \ln x_i \bigg/ \sum_{i=1}^{N} w_i \quad , \tag{S7}$$

where $\langle x\rangle_g$ is the weighted geometric mean value of a distribution of N values of x_i each with weighting w_i. In the case of Dastidar *et al.* (2007) it is the pore radius distribution that is being considered and the weighted geometric mean is R_{wgm}. In the case of Glover *et al.* (2006a; 2006b; 2006c) the distribution being considered is the grain diameter.

The big difference between the Dastidar *et al.* (2007) model and the geometric mean implementations of the RGPZ model is that the RGPZ model requires no empirical calibration, being derived analytically, while that of Dastidar et al. requires three empirical constants which were obtained by calibration with unsteady-state Klinkenberg-corrected gas permeability measurements on 150 samples with permeabilities ranging from microdarcies to darcies and porosities ranging from 0.01 to 0.30. They obtained $C_6 = 4073$, $a_6 = 1.64$, and $a_7 = 3.06$.

Huet *et al.* Model

Dastidar *et al.* (2007) and some implementations of the RGPZ model (Glover *et al.*, 2006b; 2006c) attempted to account for the full range of grain sizes in the permeability prediction. Huet *et al.* (2005) approached the same problem but from the point of view of the capillary pressure. Their approach is to relate the predicted permeability to a fit to the whole capillary pressure curve using the Brooks-Corey methodology. The consequence is a permeability prediction equation that requires knowledge of the displacement pressure P_d, Brooks-Corey parameter λ and the irreducible water saturation S_{wi} as well as the porosity ϕ, together with five empirically determined coefficients. The coefficients were found by calibrating the model against a dataset containing 89 sandstone samples which spanned a wide range of permeability (4.1 μD – 8340 mD) and porosity (0.003 – 0.34). Their measurements were made at 800 psi net confining pressure using a steady-state method and were Klinkenberg corrected. The large number of fitting parameters ensured that a good fit was possible to the calibrating dataset, but makes the method more sensitive to errors arising from its use with

other rocks than some of the other models tested in this paper. The calibration with 89 data points probably does not justify the quotation of the coefficients to between 5 and 9 significant figures. The Huet *et al.* (2005) model is given by

$$k_{HB} = C_6 \frac{1}{P_d^{a_6}} \left(\frac{\lambda}{\lambda+2} \right)^{a_7} \left(100 - S_{wi}\right)^{a_8} \phi^{a_9} \ , \tag{S8}$$

where, $C_6 = 81718.8669$, $a_6 = 1.7846$, $a_7 = 1.6575$, $a_8 = 0.5475$, and $a_9 = 1.6498$, with P_d in psi and S_{wi} in percent.

PERMEABILITY MODEL ASSESSMENT

Figure S1 shows the performance of the eight models that were judged too ineffective to be used for permeability prediction in carbonate samples together with a 1:1 line indicating a perfect prediction as well as high and low bounds representing a variance of ±2.5 (i.e., upper and lower bounds representing 2.5 times greater or less than a perfect prediction, respectively). A simple judgement concerning the goodness of prediction is that the prediction falls between the variance ±2.5 limits.

It is immediately clear that the permeabilities predicted by this set of models range over five orders of magnitude, commonly predicting permeabilities that are hundreds of times too large or too small.

Figure S1 shows that both the Katz and Thompson critical length and electrical length model provide good permeability predictions for about half of the samples, but badly underestimate the other half, with some predictions being up to 2 orders of magnitude to small.

As we predicted above, the failure of the electrical length model occurs because the electrical connectivity of the rock differs significantly from the hydraulic connectivity. Although both hydraulic and electrical flow in tight carbonates are confined to extremely thin intercrystalline pathways, narrow pore throats that are electrically open are not necessarily hydraulically patent due to the high capillary pressures that need to be overcome for flow to occur.

The Berg (2014) implementation for Fontainebleau sandstone did not predict the permeabilities of our tight carbonate samples well as expected, and should not be taken to indicate the quality of this method in general. However, our implementation of the generic

form of the Berg (2014) equation (Eq. (7) in the main paper) using the constriction factor C_s as an adjustable parameter provided good permeability predictions.
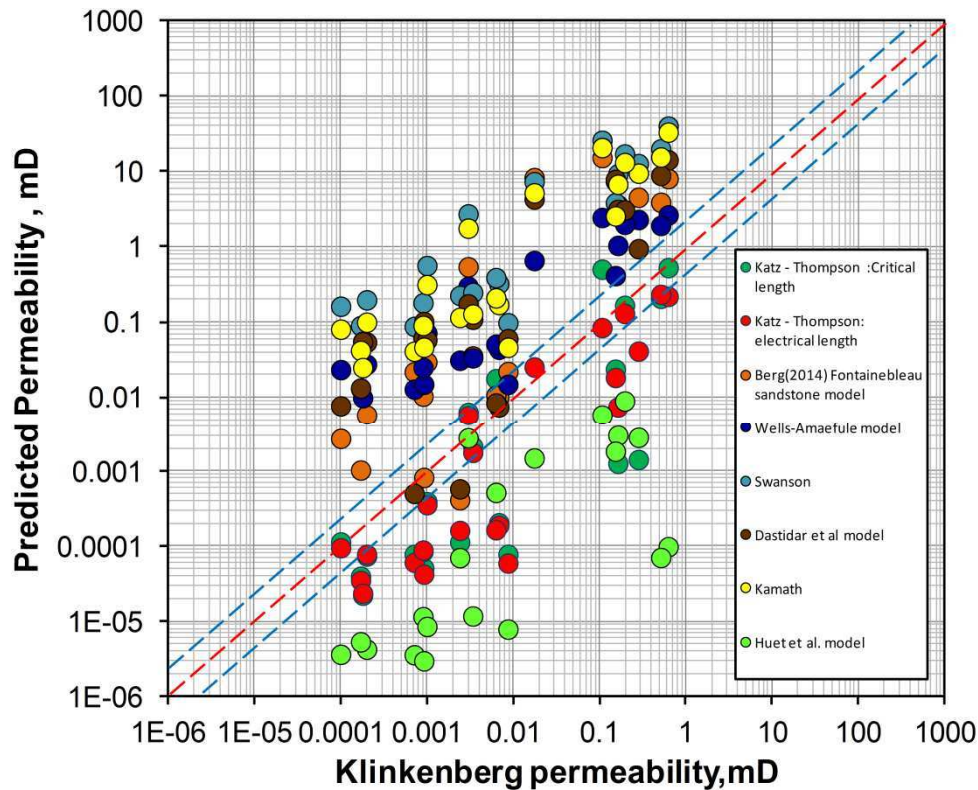

Figure S1. Predicted permeabilities as a function of measured permeabilities for the poorly calibrated models, together with a 1:1 perfect agreement and variance lines set at ±2.5. For (Huet et al model) λ=0.2 and S_{wi}=0.2.

The Poiseuille-based models generally performed badly despite the large number of parameters and coefficients they often use with exception of the Winland and Pittman models (Kolodzie, 1980; Comisky et al., 2007; Gunter et al., 2014). These models commonly overestimated the permeability by between two and three orders of magnitude. Perhaps the worst performance of all of the models was that of Swanson (1981), which provided overestimates of the permeability by between 2 and 3 orders of magnitude, and which saw only one of the samples falling within the ± 2.5 variance limits.

The Wells-Amaefule model (Wells and Amaefule, 1985) is derived from the Swanson method and would be expected to perform similarly. Wells-Amaefule model does indeed produce predictions which are similar to those of Swanson, but with a degree of overestimation reduced to between one and two orders of magnitude. This, however, is still a

very significant error, and there was only one sample for which the Wells-Amaefule model produced a prediction within the ±2.5 variance criterion.

The Kamath 'model' (Kamath, 1992) uses the same apex point as the Swanson model differing only in the dataset that it used to calibrate the model. As expected, this model also fails badly, performing very similarly to the Swanson model.

The Dastidar *et al.* (2007) model, as we have seen, is very similar to that of Winland model (Kolodzie, 1980; Comisky et al., 2007; Gunter et al., 2014) that performs well and is discussed in the main paper, differing only in the weighted geometric mean that is used to calculate the effective radius. One might, therefore, expect this model to produced similarly good results. However, the Dastidar *et al.* (2007) model did not perform well, over-estimating permeability by as much as two orders of magnitude for most of the samples tested, and obtaining a prediction within the ± 2.5 variance limits for only 18% of the samples. The reason for the difference between the Dastidar *et al.* (2007) and the Winland (Kolodzie, 1980; Comisky et al., 2007; Gunter et al., 2014) model may be important as it implies that not all of the pore size distribution contributes to the overall permeability of the rock. That in itself is not a revolutionary idea; after all the contribution to permeability made by very small pores will be rather small as result of the operation of capillary pressures and the Poiseuille equation, while the contribution to permeability made by very large pores might be rather small if the only way to flow fluid between them is so much smaller pores as was found in the carbonates with moldic porosity by Rashid *et al.* (2015). The conclusion is that the permeability will be overestimated if we incorporate permeability contributions from the very large pore sizes as well as the very small pore sizes, as occurs in the Dastidar *et al.* (2007) approach, and that a well-chosen characteristic pore radius would be more appropriate.

One of the worst predictions obtained in this study was from the use of the Huet *et al.* (2005) model. Although this is a complex model, it consistently provided predictions that fell outside the ±2.5 variance limits for all but one sample, often underestimating the permeability by 3 to 4 orders of magnitude. Variation of the lambda and irreducible water saturation has little effect on the resulting permeabilities which are strongly controlled by the displacement pressure. Displacement pressures are very high in these tight carbonates and consequently the predicted permeabilities are very low; much lower than the measured values. The Huet *et al.* (2005) model takes the entire capillary pressure curve into account when predicting the permeability. Unfortunately, entire capillary pressure curves are not available from downhole

9

measurements, so the model would be of limited practical utility even if it provided accurate permeability predictions in tight carbonates.

Ironically perhaps, the Huet *et al*. (2005) model uses as many as four variable parameters and five empirically determined coefficients. A model with a large number of adjustable parameters should be capable of producing more accurate predictions. It is instructive to note that with the exception of the Huet *et al*. (2005) model, those models which perform best in the prediction of permeability in carbonate rocks are the simplest. The Generic and RGPZ models require either no or one empirical coefficient depending on how they are used and account for 3 of the best 5 models.

CONCLUSIONS

In conclusion, all of the models described in this supplementary material do not perform well in the carbonate rocks we tested. That does not mean that they are bad models and each could perform very well in other facies types. Often, analysis of the reasons for their failure are as instructive as the reasons why other models perform well.

REFERENCES

ARCHIE, G.E. 1942. The electrical resistivity log as an aid in determining some reservoir characteristics: Transactions of the American Institute of Mechanical Engineers, 146, 54–67.

BERG, C.F. 2014. Permeability Description by Characteristic Length, Tortuosity, Constriction and Porosity. Transport in Porous Media, 103(3), pp. 381-400.

COMISKY, J.T., NEWSHAM, K., RUSHING, J.A. & BLASINGAME, T.A. 2007. A Comparative Study of Capillary-Pressure-Based Empirical Models for Estimating Absolute Permeability in Tight Gas Sands. Society of Petroleum Engineers.

DASTIDAR, R., SONDERGELD, C.H. & RAI, C.S. 2007. An Improved Empirical Permeability Estimator From Mercury Injection For Tight Clastic Rocks.

GLOVER, P.W.J. 2009. What is the cementation exponent? A new interpretation. Leading Edge (Tulsa, OK), 28(1), pp. 82-85.

GLOVER, P.W.J. 2010. A generalized Archie's law for n phases. Geophysics, 75(6), pp. E247-E265.

GLOVER, P.W.J. 2015. Geophysical Properties of the Near Surface Earth: Electrical Properties. In: Gerald Schubert (editor-in-chief) Treatise on Geophysics, 2nd edition, Vol 11. Oxford: Elsevier; 2015. p. 89-137.

GLOVER, P.W.J., ZADJALI, I.I. & FREW, K.A. 2006a. Permeability prediction from MICP and NMR data using an electrokinetic approach. Geophysics, 71(4), pp. F49-F60.

GLOVER, P.W.J., ZADJALI, I. & FREW, K. 2006b. Permeability prediction from MICP and NMR data using an electro-kinetic approach, Poster, EGU 2006, EGU06-A-01566, Vienna, 2-7 April 2006.

GLOVER, P.W.J., ZADJALI, I. & FREW, K. 2006c. A new equation for permeability prediction derived from electro-kinetic theory., Oral, GAC-MAC-SEG-SGA 2006, Abstract No. 758, Montréal,14-17 May 2006.

GUNTER, G.W., SPAIN, D.R., VIRO, E.J., THOMAS, J.B., POTTER, G., & WILLIAMS, J. 2014. Winland Pore Throat Prediction Method - A Proper Retrospect: New Examples From Carbonates and Complex Systems. Society of Petrophysicists and Well-Log Analysts SPWLA-2014-KKK, SPWLA 55th Annual Logging Symposium, 18-22 May, Abu Dhabi, United Arab Emirates.

HUET, C.C., RUSHING, J.A., NEWSHAM, K.E. & BLASINGAME, T.A. 2005. A Modified Purcell/Burdine Model for Estimating Absolute Permeability from Mercury-Injection Capillary Pressure Data. International Petroleum Technology Conference, Doha, Qatar, Nov. 21-23, Paper IPTC 10994.

KAMATH, J. 1992. Evaluation of Accuracy of Estimating Air Permeability From Mercury-Injection Data.

KATZ, A.J. & THOMPSON, A.H. 1986. Quantitative prediction of permeability in porous rock. *Physical Review B,* 34**,** 8179-8181.

KATZ, A.J. & THOMPSON, A.H. 1987a. Prediction of rock electrical conductivity from mercury injection measurements. *Journal of Geophysical Research: Solid Earth,* 92**,** 599-607.

KOLODZIE, S., JR. 1980. Analysis Of Pore Throat Size And Use Of The Waxman-Smits Equation To Determine Ooip In Spindle Field, Colorado. Society of Petroleum Engineers.

RASHID, F., GLOVER, P.W.J., LORINCZI, P., COLLIER, R., & LAWRENCE, J. 2015. Porosity and permeability of tight carbonate reservoir rocks in the north of Iraq, Journal of Petroleum Science and Engineering, 133, 147–161, http://dx.doi.org/10.1016/j.petrol.2015.05.009

SWANSON, B. F. 1981. A Simple Correlation Between Permeabilities and Mercury Capillary Pressures.

THOMEER, J.H.M. 1960. Introduction of a pore geometrical factor defined by the capillary pressure curve. *Pet. Tech***,** 73-77.

THOMPSON, A.H., KATZ, A.J., & RASCHKE, R.A. 1987. Estimation of Absolute Permeability from Capillary Pressure Measurements. Paper SPE 16794 presented at the 1987 SPE Annual Technical Conference and Exhibition, Dallas, TX, Sept. 27-30.

WELLS, J.D. & AMAEFULE, J.O. 1985. Capillary Pressure and Permeability Relationships in Tight Gas Sands. Society of Petroleum Engineers.